AFIT/GA/ENY/95D-01

NUMERICAL STUDY OF A TRANSPIRATION COOLED ROCKET NOZZLE

THESIS

Jay A. Landis, B.S.

AFIT/GA/ENY/95D-01

Approved for public release; distribution unlimited

Disclaimer Statement

The views expressed in this thesis are those of the author and do not reflect the official policy or position of the Department of Defense or the U. S. Government.

AFIT/GA/ENY/95D-01

NUMERICAL STUDY OF A TRANSPIRATION COOLED ROCKET NOZZLE

THESIS

Presented to the Faculty of the Graduate School of Engineering

of the Air Force Institute of Technology

Air University

In Partial Fulfillment of the

Requirements for the Degree of

Master of Science in Astronautical Engineering

Jay A. Landis, B.S.

Captain, USAF

December 1995

Preface

This paper represents an attempt to characterize the steady state effects of transpiration cooling within a porous rocket nozzle wall. Its intent is to go beyond the boundary condition problem to better understand the effects within the porous wall. Along the way, I learned a lot from many different people and I owe them all a debt of gratitude for their patience and assistance.

The person at the top of the list is my thesis advisor, Lt. Col. Jerry Bowman. His patience with my questions and willingness to help at any time deserves recognition. Next I have to thank Mr. Don Rousar at Aerojet. He provided answers to many of my basic questions regarding the transpiration cooling process. He also provided me with many resources and references. Next I wish to thank Ms. Kim Parks from Marshall Space Flight Center for the technical data on the SSME MCC. Also, I wish to thank Mr. Dan Griesen at Aerojet for the combustion product properties. Without these peoples' help, this project would not have been completed. Finally, all my love, gratitude, and thanks go to the two greatest gifts I have ever been given, my wife, Nancy, and daughter, Chloe.

Jay Landis

Table of Contents

List of Figures

List of Tables

List of Symbols

Symbol	Description	Units
A	Flow cross-sectional area	m^2
BR	Blowing ratio	
c_p	Specific heat at constant pressure	J/(kg*K)
D	Diameter	m
$\dot{E}$	Rate of energy change	W
h	Heat transfer coefficient	$W/(m^2*K)$
i	Enthalpy	J/kg
k	Thermal conductivity	W/(m*K)
K	Permeability	
L	Thickness of the porous wall	m
$\dot{m}$	Mass flow rate	kg/s
M	Mach number	
P	Pressure	N/m^2
Per	Wetted perimeter	m
Pr	Prandtl number	
q''	Heat flux	W/m^2
r	Radius	m
R	Recovery factor	

Re	Reynold's number	
t	Time	s
T	Temperature	K
u	Velocity	m/s
ε	Void fraction or porosity	
γ	Ratio of specific heats	
μ	Viscosity	kg/(m*s)
σ	Symbol used to represent complicated term in Bartz' Eqn	
ρ	Density	kg/m^3
ω	Viscosity-Temperature exponent	

Subscripts

0	Total conditions
aw	Adiabatic wall
b	Bulk temperature conditions
c	Coolant
cl	Coolant liquid
cs	Cold side
curv	Curvature
f	Film
g	Gas

h	Hydraulic
i	Point of interest
l	Liquid
p	Particle
s	Solid
surf	Surface
t	Nozzle throat
WC	Cold wall
WH	Hot wall

Abstract

This study proved that transpiration cooling provides a better cooling scheme than regenerative cooling for long operating duration liquid-fueled rocket engine nozzles. This proof was made on the basis of maximum wall temperature. This study compared transpiration cooling to regenerative cooling in the throat region of the Space Shuttle Main Engine Main Combustion Chamber. The study also analyzed the effects of porosity, solid thermal conductivity, and porous sphere size on a porous wall made of packed spheres. The transpiration cooled nozzle operated 35% cooler than a regeneratively cooled nozzle, but the temperature gradient at the hot gas surface was 72 times greater than the regeneratively cooled nozzle.

NUMERICAL STUDY OF A TRANSPIRATION COOLED ROCKET NOZZLE

I. Introduction

1.1 Background

Future space systems are looking toward higher thrust, longer operating duration, more reliable, more reusable systems. To increase thrust efficiency, combustion chambers must operate at higher chamber pressures and temperatures. This requires sufficient cooling to maintain the combustion chamber material within acceptable temperature limits either to prevent failure or increase cycle life. The peak heat flux in a rocket nozzle occurs near the throat, therefore the true measure of a cooling system is how well it operates in the throat region (Hill and Peterson, 1992:550).

The currently accepted norm for cooling the nozzles of long operating duration, liquid-fueled rocket engines is regenerative cooling (Mueggenburg and others, 1992:2). Regenerative cooling, or forced convection cooling, passes cold fuel at high velocities through small channels imbedded in the nozzle wall to absorb the heat from the hot wall and to preheat the fuel (Hill and Peterson, 1992:541). Another method to cool the rocket nozzle is transpiration cooling. Transpiration cooling is the injection of a cooling fluid through a porous wall material over a relatively large surface area.

1.2 Thesis Statement

Transpiration cooling provides a better cooling scheme than regenerative cooling for a liquid-fueled, long operating duration rocket nozzle.

1.3 Justification

The most technologically advanced example of regenerative cooling used in a reusable, liquid-fueled, high chamber pressure rocket engine is the Space Shuttle Main Engine (SSME). Even though regenerative cooling was originally chosen for the SSME, after several operational flights it was discovered that regenerative cooling does not provide enough cooling for the SSME to meet cycle life requirements. Thermally induced stresses caused surface defects which increased the number of between-launch service repairs. Two identified failure modes resulted in cracks in the surface of the SSME main combustion chamber (MCC) (Murphy and others, 1986:2; Quentmeyer, 1990:1).

Regenerative cooling also creates other problems. One problem is the pressure drop that occurs in the small coolant channels. Regenerative cooling requires high velocity coolant flow through very small channels to increase heat transfer enough to cool the hot wall. This causes a large pressure drop through the coolant channels. This pressure drop creates one of two problems. Either the fuel turbopump requires a higher discharge pressure to maintain the same combustion chamber pressure, or the chamber pressure must decrease to make up for the pressure drop. Furthermore, higher turbopump discharge pressures cause a decrease in life of the turbopump (May and others, 1990:1).

Another problem with regenerative cooling is that it requires very thin hot gas wall thicknesses. This is done to prevent steep temperature gradients that cause thermal strain and decreased cycle life. Unfortunately, the desired wall thicknesses approach the tolerances of conventional machining processes (Mueggenburg and others, 1992:2).

Because of these problems, the National Aeronautics and Space Administration (NASA) and the Air Force Advanced Launch System (ALS) began looking for high reliability, low cost cooling schemes for proposed future booster designs. A study in 1990 summarized several new cooling techniques and pointed out transpiration cooling as a promising new method (Quentmeyer, 1990:5-6).

Work has been done at the Air Force Institute of Technology (AFIT) to experimentally explore the effects of transpiration cooling on heat transfer to the wall of a supersonic nozzle (Lenertz, 1994; Keener, 1994; Chen, 1995). The most important result of these studies was a simple mathematical expression that quantifies the decrease in heat transfer to the hot gas side wall due to the injection of the coolant (Chen, 1995:1).

1.4 Purpose

The purpose of this thesis is to prove that transpiration cooling provides a better cooling scheme than regenerative cooling for a liquid-fueled, long operating duration rocket nozzle. To prove this fact, the author chose maximum wall temperature and maximum temperature gradient as the figures of merit for cooling performance. A cooling scheme that provides the lowest wall temperature with the lowest temperature gradient would be considered the best cooling scheme.

This study also characterizes the relative importance of different geometric and thermodynamic properties of the wall material. These properties are the porosity, the void fraction of the porous material, and the thermal conductivity, the material's ability to transfer heat through the solid. Another parameter of interest is the blowing ratio. The blowing ratio is defined as the mass flow per unit area of injected fluid divided by the mass flow per unit area of free stream hot gas. Or in mathematical terms, the blowing ratio is

$$BR = \frac{\rho_l u_l}{\rho_g u_g} \tag{1}$$

where BR is the blowing ratio, ρ_l is the density of the injected coolant, u_l is the uniform velocity of the injected coolant at the porous surface, ρ_g is the density of the free stream hot gases, and u_g is the uniform free stream velocity of the hot gases (Lenertz, 1994:2). The pressure difference across the porous nozzle wall of a transpiration cooled nozzle determines the blowing ratio. By studying the relative importance of varying these three parameters, the design engineer will be able to select the appropriate porosity, material to construct the porous nozzle wall, and blowing ratio for a given problem.

1.5 Methodology

The author developed a finite difference numerical model of the heat transfer through the porous wall. This model treats the transpiration coolant flow and heat transfer as one dimensional. This assumption is justified through the advancement of platelet technology. Platelet technology involves photo-etching channels into very thin layers of material and bonding these layers together to form a composite structure. These tiny channels provide accurate metering of the flow to meet either a specific pressure or heat flux profile without two or three dimensional coolant flow effects (Mueggenburg and others, 1992:1-2). The one dimensional heat transfer assumption is justified due to the relative magnitudes of the temperature gradients. The temperature gradient along the nozzle wall does not approach the 4×10^5 K/m gradient that occurs within the nozzle wall, therefore two dimensional effects can be neglected.

The author chose to represent the porous nozzle wall as a packed bed of spheres with the transpiration coolant constrained to flow in only one direction. Since the transpiration coolant follows a tortuous path through both the platelet wall and the packed

bed of spheres wall and the coolant flow is constrained to flow in only one direction, the packed bed of spheres model is valid. Five different regular geometrical arrangements of spherical particles were used to represent the porous material construction. This allowed computation of porosity and solid surface area exposed to fluid flow. The solid surface area is critical in linking the heat transfer between the solid and the coolant as it flows through the porous solid. In addition, the use of spheres allowed the author to use the heat transfer equations for heat transfer from a gas to a packed bed of spheres.

Since the SSME MCC is the most technologically advanced, operational example of regenerative cooling, the author chose it as the standard against which all transpiration cases should be judged. The SSME MCC nozzle and coolant channel dimensions were used in the heat transfer equations. Because hydrogen is already used as the cooling fluid in the SSME MCC at the throat region, hydrogen was chosen as the transpiration coolant fluid. Additionally, hydrogen would be a good coolant for transpiration cooling because it has a low molecular weight, which is desirable for a higher engine specific impulse (Bowman and others, 1994:20). At nozzle pressures and temperatures, the hydrogen coolant is a supercritical fluid that behaves like an ideal gas. The hydrogen is neither a liquid or a gas, it is in a state between the two. Throughout this thesis, the terms fluid, liquid and gas are used interchangeably to refer to the transpiration coolant.

Five different thermal conductivities representing five different solid materials were used in the parameter study. The values of these thermal conductivities represent the range from insulators to very good thermal conductors. Five different pressure differences were used to obtain a spread of blowing ratios. An additional parameter in the porous material is the sphere size used to make the porous solid. There were three sphere radius sizes chosen.

The numerical model was built in a modular design. Each subroutine was tested independently. The solid and liquid subroutines were validated against known exact solutions. Once these subroutines were validated, they were combined to create the complete model. The model was run comparing each of the porosities against each of the thermal conductivities at various pressure differences to generate a spread of blowing ratios. Finally, the maximum temperatures and maximum temperature gradients were plotted against blowing ratio to observe trends as porosity and thermal conductivity vary.

II. Numerical Model

This chapter provides descriptions of the equations used in the numerical model. The chapter begins with an overview of the heat transfer processes within a porous wall and a statement of the energy equations for the porous solid and liquid transpiration coolant. The next two sections describe the equations that govern the boundary heat flux conditions. The fourth section in this chapter describes the heat transfer that takes place between the porous solid and liquid coolant. The fifth section describes the source of the properties used in the model. The final section of this chapter gives a brief overview of the program structure. The model was programmed in FORTRAN and the code is provided in Appendix B.

2.1 Transpiration Cooling Overview

The various heat and energy transfer mechanisms involved in transpiration cooling are illustrated in Figure 1. The two mechanisms of heat transfer used in this study are conduction and convection. One dimensional conduction heat transfer is described by Fourier's Law

$$q'' = -k\frac{dT}{dx} \tag{2}$$

where q'' is the heat flux due to conduction in watts per square meter, k is the thermal conductivity of the material, and $\frac{dT}{dx}$ is the temperature gradient within the material (Incropera and DeWitt, 1990:4). Convection heat transfer between a solid of temperature, T_s, and a liquid of temperature, T_l, is described by Newton's Law of Cooling

$$q'' = h(T_s - T_l) \tag{3}$$

where q'' is the heat flux due to convection in watts per square meter, and h is the heat transfer coefficient in watts per square meter per degree Kelvin (Incropera and DeWitt, 1990:8). Energy is also transferred through the transpiration coolant by the work done by the pressure forces on the fluid and the advection of kinetic and internal energy by the fluid (Incropera and DeWitt, 1990:326-334).

The heat transfer and energy mechanisms are combined to form the energy equations for the solid and the liquid. Appendix A contains the derivations of the energy equations, but the final forms are provided here for the reader. The solid energy equation assumes (1) the only mode of heat transfer through the solid is by conduction, and (2) the only loss of energy is to the transpiration coolant. The energy equation for the porous solid used in this model is given in Equation (4).

$$k_s \frac{d^2 T_s}{dx^2} - \frac{h_{cl} A^* (T_s - T_l)}{A dx} = \rho_s c_{p_s} \frac{dT_s}{dt} \tag{4}$$

The first term in the solid energy equation represents the conduction through the solid. The second term describes the heat transfer from the solid to the liquid, where A^* is the surface area of the solid exposed to the transpiration coolant and A is the cross sectional area of the nozzle wall exposed to the transpiration coolant flow. The term on the right hand side of the energy equation is the transient term and is only required for obtaining convergence to the steady state solution.

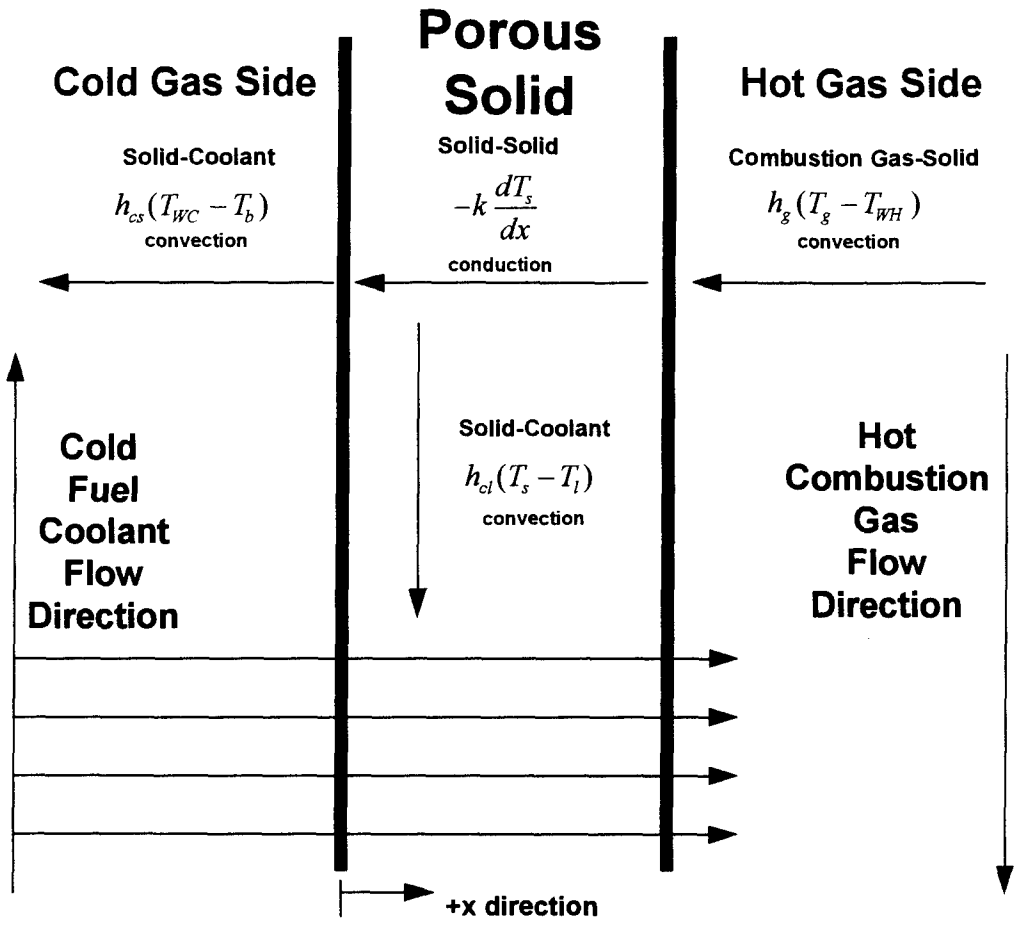

Figure 1. Heat Transfer Mechanisms Within a Porous Solid

The liquid energy equation assumed: (1) the only work done on the fluid by external forces is by pressure forces, (2) the only means of energy transfer across the control volume is by conduction and advection, (3) the temperature gradient term dominates the heat transfer and the kinetic energy term can be neglected, (4) the coolant behaves like an ideal gas, and (5) the heat transfer from the porous solid to the coolant is

the only energy gain. The energy equation for the liquid transpiration coolant used in this model is given in Equation (5).

$$k_l \frac{d^2 T_l}{dx^2} + \frac{h_{cl} A^* (T_s - T_l)}{A_l dx} - \rho_l u_l c_{p_l} \frac{dT_l}{dx} = 0 \tag{5}$$

The first term in the liquid energy equation is the conduction through the liquid. The second term describes the amount of energy that is transferred from the solid to the liquid and is considered an energy gain. The third term describes the advection of energy through the liquid and is considered an energy loss.

The differential energy equations were converted to explicit finite difference forms so they could be solved numerically. The TSOLID subroutine solves for the solid temperature profile and the TLIQUID subroutine calculates the liquid temperature profile. Before the energy equations could be solved numerically, the boundary conditions on the hot gas and cold gas sides must be established.

2.2 Hot Gas Side Heat Transfer

The heat transfer on the hot combustion gas side of the nozzle wall comes from convection and radiation. Because the heat transfer correlation used includes radiation effects, the author did not add the radiation boundary condition to the energy equation (Bartz, 1965:16-17). Newton's law of cooling states that the heat flux due to convection from a hot gas to a solid surface takes the form

$$q'' = h_g (T_g - T_{WH}) \tag{6}$$

where h_g is the heat transfer coefficient, T_g is the fluid temperature, and T_{WH} is the solid wall surface temperature at the point of interest. For high speed flow, the fluid temperature, T_g, is replaced with the adiabatic wall temperature, T_{aw}, due to viscous heating in the turbulent boundary layer. This adiabatic wall temperature can be found from the recovery factor, R, represented by

$$R = \mathrm{Pr}^{1/3} = \frac{T_{aw} - T_g}{T_{o_g} - T_g} \tag{7}$$

where T_{o_g} is the stagnation temperature of the fluid, and T_g is the free stream temperature of the fluid (Kreith and Bohn, 1986:586). The Prandtl number, Pr, of the fluid is evaluated at the film temperature, T_f

$$T_f = T_{WH} + 0.23(T_g - T_{WH}) + 0.19(T_{aw} - T_{WH}) \tag{8}$$

(Hill and Peterson, 1992:550). The FINDTAW subroutine solves for the adiabatic wall temperature.

The last term needed is the heat transfer coefficient, h_g. An expression derived by Bartz for the heat transfer coefficient from the hot combustion gases to the nozzle wall without transpiration cooling effects is given in Equation (9).

$$h_{g0} = \left[\frac{0.026}{D_t^{0.2}} \left(\frac{\mu_g^{0.2} c_{p_g}}{\mathrm{Pr}_g^{0.6}} \right)_0 \left(\frac{\dot{m}_g}{A_t} \right)^{0.8} \left(\frac{D_t}{r_{curv}} \right)^{0.1} \right] \left(\frac{A_t}{A_i} \right)^{0.9} \sigma \tag{9}$$

where h_{g0} represents heat transfer without blowing, D_t and A_t are the nozzle throat diameter and area respectively, r_{curv} is the radius of curvature of the nozzle in the plane that contains the nozzle axis, $\dot{m}_g$ is the mass flow rate of the combustion products, A_i is the nozzle cross sectional area of interest, and the 0 subscript implies that these properties are evaluated at stagnation conditions (Bartz, 1965:35). The σ term is given by

$$\sigma = \frac{1}{\left[\frac{1}{2}\frac{T_{WH}}{T_{0_g}}\left(1+\frac{\gamma-1}{2}M^2\right)+\frac{1}{2}\right]^{0.8-0.2\omega}\left[1+\frac{\gamma-1}{2}M^2\right]^{0.2\omega}} \tag{10}$$

where γ is the ratio of specific heats of the combustion products, M is the local Mach number of the combustion gases, and ω is the exponent of the viscosity-temperature relation, $\mu \propto T^{\omega}$. For diatomic gases, $\omega = 0.6$ (Hill and Peterson, 1992:550). Since the combustion products are not all diatomic gases, the author plotted the viscosity of the combustion products at the nozzle throat conditions against temperature and obtained the value of $\omega = 0.875$. The approximate error in using this correlation is 2% but can be as high as 30% near the throat (Bartz, 1965:59).

Lenertz and Chen (1994; 1995) discovered that there is a decrease in heat flux from a hot gas to the nozzle wall if transpiration cooling is used through the nozzle wall. An objective in transpiration cooling is to maximize the heat reduction, while minimizing the disturbance to the primary flow boundary layer (Sucec, 1985:821). If the blowing is too great, the boundary layer grows and the effective nozzle throat and nozzle exit areas are decreased causing a decrease in performance. Even at low blowing ratios, Keener (1994:65) found there is a 47% increase in the boundary layer with transpiration cooling although much of this increase was due to the rough surface. The range of blowing ratios

considered by Chen was from -0.0002 to 0.0117, where negative values indicate suction and positive values indicate blowing. Lenertz and Chen (1994; 1995) used a two dimensional Mach 2 nozzle in the AFIT shock tube to measure the effect of transpiration cooling on heat transfer. Chen created a mathematical expression that related the blowing heat transfer coefficient to the non-blowing heat transfer coefficient in Equation (11).

$$\frac{h_g}{h_{g0}} = (1 - 38.0 * BR) \tag{11}$$

where h_g is the heat transfer including blowing effects, h_{g0} is heat transfer without blowing, and BR is the blowing ratio (Chen, 1995:4.11). Since the maximum blowing ratio valid for Chen's correlation was 0.0117 (1995:1), the author chose to limit the scope of blowing ratios to less than 0.01. The HOTGAS subroutine calculates the hot gas side heat transfer coefficient including transpiration effects.

2.3 Cold Gas Side Heat Transfer

Like the hot gas side, the heat transfer on the cold gas side is defined by convection. The heat flux from convection from a hot solid to a cold gas takes the form

$$q'' = h_{cs}(T_{WC} - T_b) \tag{12}$$

where h_{cs} is the heat transfer coefficient, T_b is the bulk fluid temperature, and T_{WC} is the solid wall surface temperature. Since T_{WC} is not known initially, the author chose to use an expression for the heat transfer coefficient that accounts for large temperature differences between T_b and T_{WC}, and the cold fluid is in turbulent conditions. The expression used is given in Equation (13) (Incropera and DeWitt, 1990:496).

$$h_{cs} = \frac{0.027 k_l}{D_h} \mathrm{Re}_{D_h}^{4/5} \mathrm{Pr}^{1/3} \left(\frac{\mu_{lb}}{\mu_{l_{surf}}} \right)^{0.14} \tag{13}$$

where D_h is the coolant channel hydraulic diameter, Re_{D_h} is the Reynolds number defined as

$$\mathrm{Re}_{D_h} = \frac{4\dot{m}_c}{\mu_{lb} Per_h} \tag{14}$$

where $\dot{m}_c$ is the mass flow rate of the coolant in the coolant channel, and Per_h is the coolant channel wetted perimeter. In Equation (13) all properties are evaluated at the coolant bulk temperature, T_b, except $\mu_{l_{surf}}$, which is evaluated at the solid surface temperature, T_{WC}. The approximate error in using this correlation is 25% (Incropera and DeWitt, 1990:496). The HCOOLSIDE subroutine calculates the heat transfer coefficient, h_{cs}.

2.4 Packed Bed of Spheres Heat Transfer

The only remaining unknown in the energy equations is the heat transfer coefficient for convection between the porous solid and the transpiration coolant. Since the porous solid is assumed to be made of a packed bed of very small spheres, an expression for the heat transfer coefficient, h_{cl}, is given in Equation (15) (Whitaker, 1972:366-368).

$$h_{cl} = \frac{k_l}{2r_p} \frac{1-\varepsilon}{\varepsilon} \left(0.5 \mathrm{Re}_{r_p}^{1/2} + 0.2 \mathrm{Re}_{r_p}^{2/3} \right) \mathrm{Pr}^{1/3} \tag{15}$$

where k_l is the thermal conductivity of the coolant, r_p is the sphere radius of the porous solid material, Pr is the Prandtl number of the fluid, and Re_{r_p} is the Reynolds number defined by

$$\mathrm{Re}_{r_p} = \frac{2 r_p \dot{m}_l}{\mu_l \varepsilon (1-\varepsilon)} \tag{16}$$

where $\dot{m}_l$ is the mass flow rate of the coolant through the porous solid, and ε is the porosity of the solid. All liquid properties in Equation (15) are evaluated at the average between the bulk liquid temperatures entering and exiting the porous wall (Whitaker, 1972:366-368).

Since the flow velocity of the coolant is relatively slow in the porous solid, the coolant is assumed to be incompressible. Darcy's law relates the mass flow rate of an incompressible liquid to the pressure gradient in the liquid in Equation (17) (Brennan and Kroliczek, 1979:25).

$$\frac{dP}{dx} = -\frac{\mu_l \dot{m}_l}{K \rho_l A_l} \tag{17}$$

In Equation (17), $\frac{dP}{dx}$ is the pressure gradient through the porous solid, $\dot{m}_l$ is the mass flow rate of the coolant through the porous solid, μ_l and ρ_l are the viscosity and density of the coolant, and K is the permeability of the solid. For a packed bed of spheres, the permeability, K, is defined in Equation (18) (Brennan and Kroliczek, 1979:118).

$$K = \frac{(2 r_p)^2 \varepsilon^3}{150 (1-\varepsilon)^2} \tag{18}$$

Since the heat transfer coefficient, h_{cl}, is evaluated at the average temperature, the viscosity and density should be evaluated at the same average temperature. Therefore all the terms are constant throughout the porous solid and Equation (17) simplifies to

$$\frac{(P_b - P_t)}{L} = \frac{\dot{m}_l \mu_l}{K \rho_l} \tag{19}$$

where P_b is the coolant line pressure, P_t is the nozzle static throat pressure, and L is the thickness of the porous wall. This equation can be rearranged to obtain $\dot{m}_l$ in Equation (20).

$$\dot{m}_l = \frac{(P_b - P_t) K \rho_l}{L \mu_l} \tag{20}$$

The HCOOL subroutine calculates the heat transfer coefficient, h_{cl}.

2.5 Properties

To calculate the heat transfer at the hot gas side of the porous wall, the author needed thermodynamic properties for the hot combustion gases at various temperatures. The combustion product properties came from Mr. Dan Griesen at AEROJET corporation in Sacramento, California. The properties were generated by a computer code from NASA called TRAN72. Mr. Griesen provided the author with the output from a 6:1 fuel to oxidizer combustion mixture at 20.68 MPa and 3656.7 K combustion temperature. These conditions represent 100% thrust of a SSME. Curve fits were made for these hot gas properties. The HOTGASPROP subroutine contains the curve fits for the combustion product properties (Griesen, 1995).

Likewise, the author needed various thermodynamic properties for hydrogen at varying pressures and temperatures to calculate the packed bed of sphere heat transfer and the cold gas side heat transfer. The hydrogen coolant properties came from Mr. Don Rousar at AEROJET corporation in Sacramento, California. They are from an internal report generated by AEROJET for use in their calculations. Curve fits were made for the pertinent hydrogen properties. The H2PROP subroutine contains the curve fits for the hydrogen properties (Rousar, 1995).

The SSME MCC geometrical dimensions and the NARloy-Z properties were obtained from Ms. Kim Parks at Marshall Space Flight Center in Huntsville, Alabama. She provided technical drawings of the SSME MCC and plots of NARloy-Z thermal conductivity. She also provided a computer generated output of several SSME key properties such as, coolant mass flow rate through the coolant channels, and combustion product mass flow rate through the nozzle throat (Parks, 1995).

The thermal conductivity of a porous solid is not simply the thermal conductivity of the solid material. The effective thermal conductivity of a saturated porous material comprised of a packed bed of spheres is given by

$$k_s = \frac{k_l\left[\left(2k_l + k_w\right) - 2(1-\varepsilon)(k_l - k_w)\right]}{\left[2k_l + k_w + (1-\varepsilon)(k_l - k_w)\right]} \tag{21}$$

where k_s is the effective thermal conductivity of the porous material, k_l is the thermal conductivity of the liquid, k_w is the thermal conductivity of the solid material, and ε is the porosity of the material (Chi, 1976:50).

2.6 Program Structure

The two subroutines, TLIQUID and TSOLID, numerically evaluate the energy equations for the liquid coolant and porous solid. Since the two energy equations are tied through the internal convection term, $\frac{h_{cl}A^*(T_s - T_l)}{Adx}$, the two temperature distributions have to be solved iteratively. The INPUT subroutine reads in the initial parameters for porosity, solid thermal conductivity, coolant channel pressure, and solid surface area exposed to coolant flow within the solid. The INPUT subroutine also specifies an initial temperature profile through the porous wall for both the liquid and solid. The TLIQUID subroutine uses a backward differencing technique and the solid temperature profile to calculate a new liquid temperature profile through the porous wall. The TSOLID subroutine uses the updated liquid temperature profile and a forward differencing technique to obtain a new solid temperature profile through the wall. At each point a new time step is calculated based upon the stability criterion. After calculating the two profiles, the new temperature values were compared to values from the previous time step. Once the difference was less than a specified tolerance, the solutions had converged. After both temperature profiles converge, the OUTPUT subroutine is called to write the temperature profiles to a specified filename.

III. Model Validation

This chapter provides a discussion of the validation methods used for each of the subroutines within the numerical model. The chapter begins with a brief description of the validation of property and heat transfer coefficient subroutines. The next section describes the results of the various test cases used to validate the TSOLID subroutine. The chapter ends with a description of the TLIQUID validation and results.

3.1 Validation of Property and Heat Transfer Coefficient Subroutines

The author verified the H2PROP, HOTGASPROP, HCOOLSIDE, HOTGAS, HCOOL, and FINDTAW subroutines by hand calculations and comparison with property data. All subroutines generated correct results.

3.2 TSOLID Validation

The author used three incremental steps to validate the TSOLID subroutine. In validating the TSOLID subroutine, energy transfer to the liquid was ignored and the solid was treated with zero porosity. The first step was to test the model with two fixed boundary temperatures. The two temperatures were 138.89 K and 3656.7 K. The exact temperature profile in a planar wall with no internal heat generation is a straight line governed by Equation (22) (Incropera and DeWitt, 1990:81).

$$T_s(x) = T_{WC} + \frac{(T_{WH} - T_{WC})x}{L} \tag{22}$$

where $T_s(x)$ is the solid temperature as a function of distance, x, through the wall, T_{WC} is the cold wall temperature, T_{WH} is the hot wall temperature, and L is the total thickness of

the wall. The model generated the profile shown in Figure 2. As the reader can see, the solid temperature profile is linear, beginning and ending at the appropriate boundary temperatures.

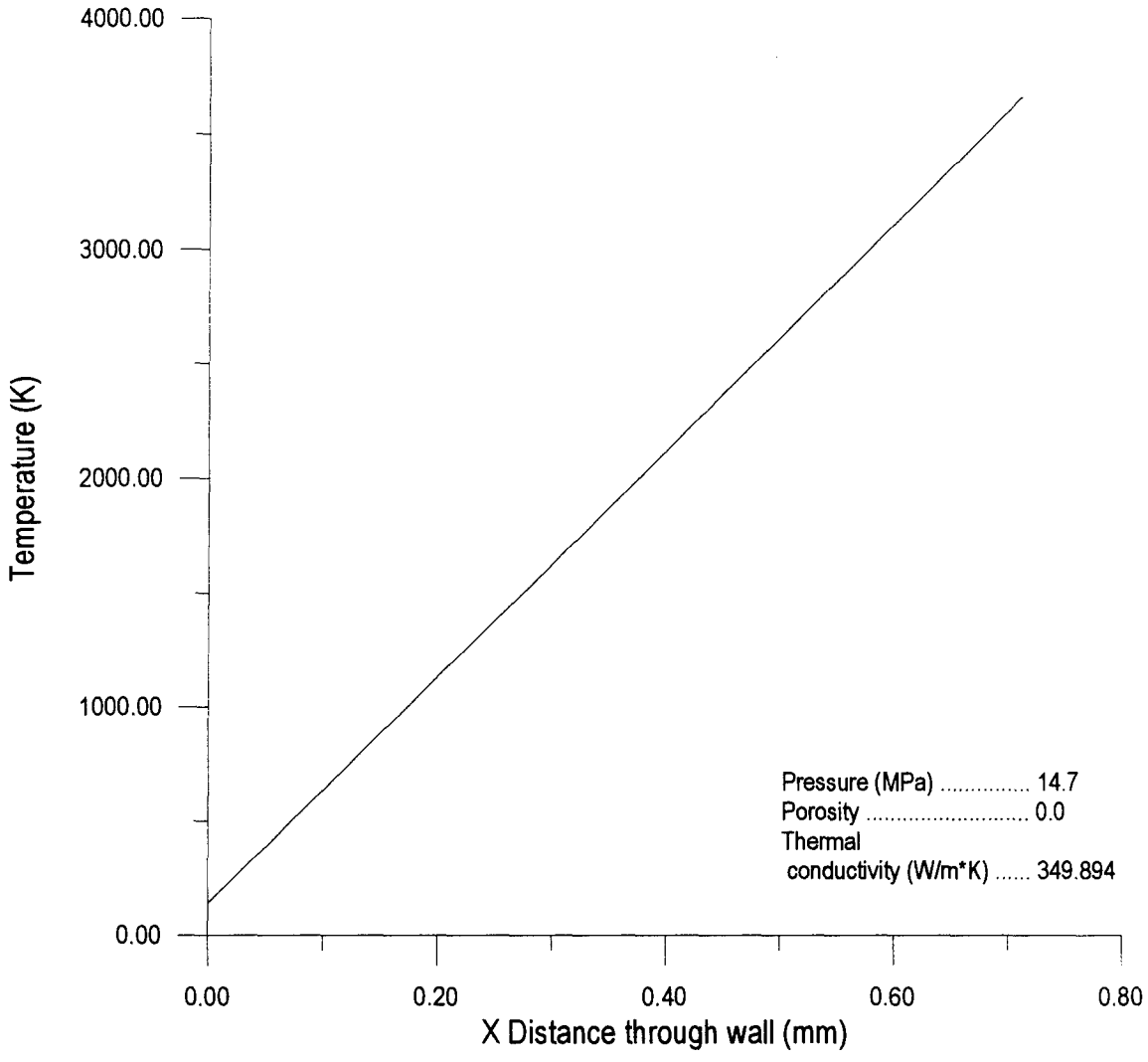

Figure 2. Fixed Temperature Boundary Condition Solid Temperature Profile

The second step was to impose two fixed convection boundary conditions. The adiabatic wall temperature, T_{aw}, was fixed at 3656.7 K, the hot side heat transfer coefficient, h_g, was fixed at 20,000 W/(m^2*K), the cold side heat transfer coefficient, h_{cs}, was fixed at 10,000 W/(m^2*K), and the bulk temperature of the coolant, T_b, was held constant at 138.89 K. The exact temperature profile is a straight line governed by Equation (22). In this case, the temperatures T_{WH} and T_{WC} are unknown. Using the heat flux correlations shown in Sections 2.2 and 2.3, and knowing that the heat flux into the wall equals the heat flux out of the wall, the reader can see that T_{WH} and T_{WC} are functions of T_{aw} and T_b. The hot wall and cold wall temperatures are calculated using the equations below (Incropera and DeWitt, 1990:83).

$$q'' = \frac{T_{aw} - T_b}{\frac{L}{k_s} + \frac{1}{h_g} + \frac{1}{h_{cs}}} \tag{23}$$

$$T_{WH} = T_{aw} - \frac{q''}{h_g} \tag{24}$$

$$T_{WC} = T_b + \frac{q''}{h_{cs}} \tag{25}$$

The TSOLID model generated a solid temperature profile that matched the exact solution. Some select temperature values are listed in Table 1.

TABLE 1
FIXED CONVECTIVE HEAT TRANSFER COEFFICIENT TEST CASE RESULTS

X Location millimeters	Exact Values K	Computed Values K
0	2452.752	2452.377
0.305816	2472.966	2472.599
0.7112	2499.774	2499.412

The third step was to run the model with realistic heat transfer coefficients calculated from the same material, combustion, and coolant properties as the SSME MCC. The model results were compared to the actual measured SSME MCC temperature values. The measured values for the SSME MCC wall temperatures were 838.7 K on the hot gas side and 505.4 K on the cold gas side (Cook and Coffey, 1973:8). These results are shown in Figure 3. The dashed lines represent the maximum error caused by the heat transfer correlations utilizing the ±25% error on the cold gas side and the ±2% error on the hot gas side. As the reader can see, considering the possible error, the model generates values very close to experimental results. Based upon these results, the author is confident the boundary condition heat transfer equations and the TSOLID model generate valid results.

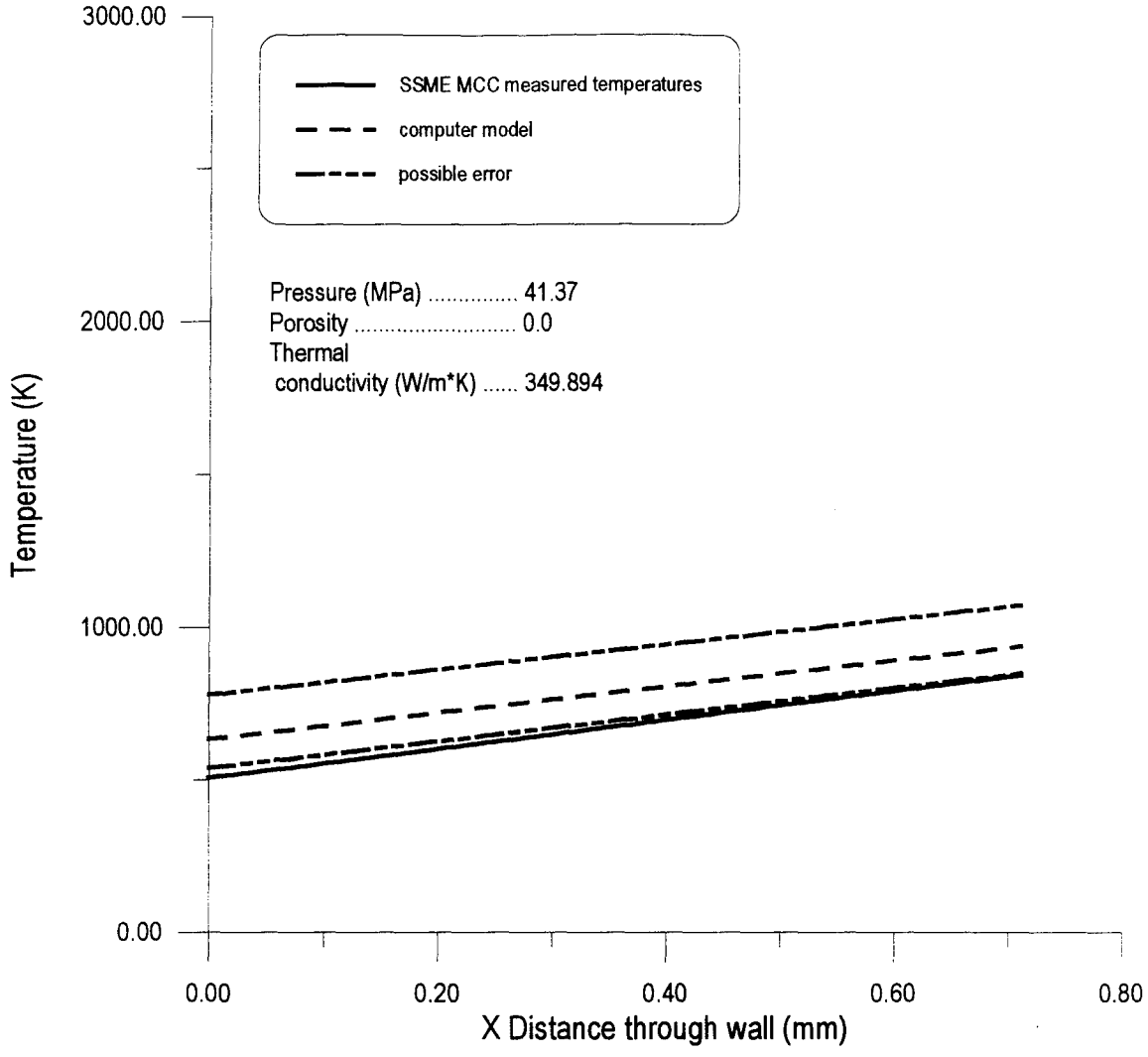

Figure 3. Regeneratively Cooled Model vs. Experimental Results

3.3 TLIQUID Validation

The exact solution for constant liquid property flow through a packed bed of spheres held at a constant wall temperature is

$$\frac{T_s - T_{l,out}}{T_s - T_{l,in}} = \exp\left(-\frac{h_{cl} A^*}{\dot{m}_l c_{p_l}}\right) \tag{26}$$

where T_s is the solid temperature, $T_{l,in}$ is the inlet bulk temperature, $T_{l,out}$ is the exit bulk temperature, h_{cl} is the average heat transfer coefficient, $\dot{m}_l$ is the mass flow rate of coolant through the bed, A^* is the solid surface area exposed to the fluid, and c_{p_l} is the specific heat of the fluid (Incropera and DeWitt, 1992:440). Various grid sizes were used to plot the computed TLIQUID temperature profile for a constant wall temperature of 2000 K and constant hydrogen properties at 138.89 K and 12.0 MPa. The liquid temperature profiles for each of the grid sizes are plotted in Figure 4.

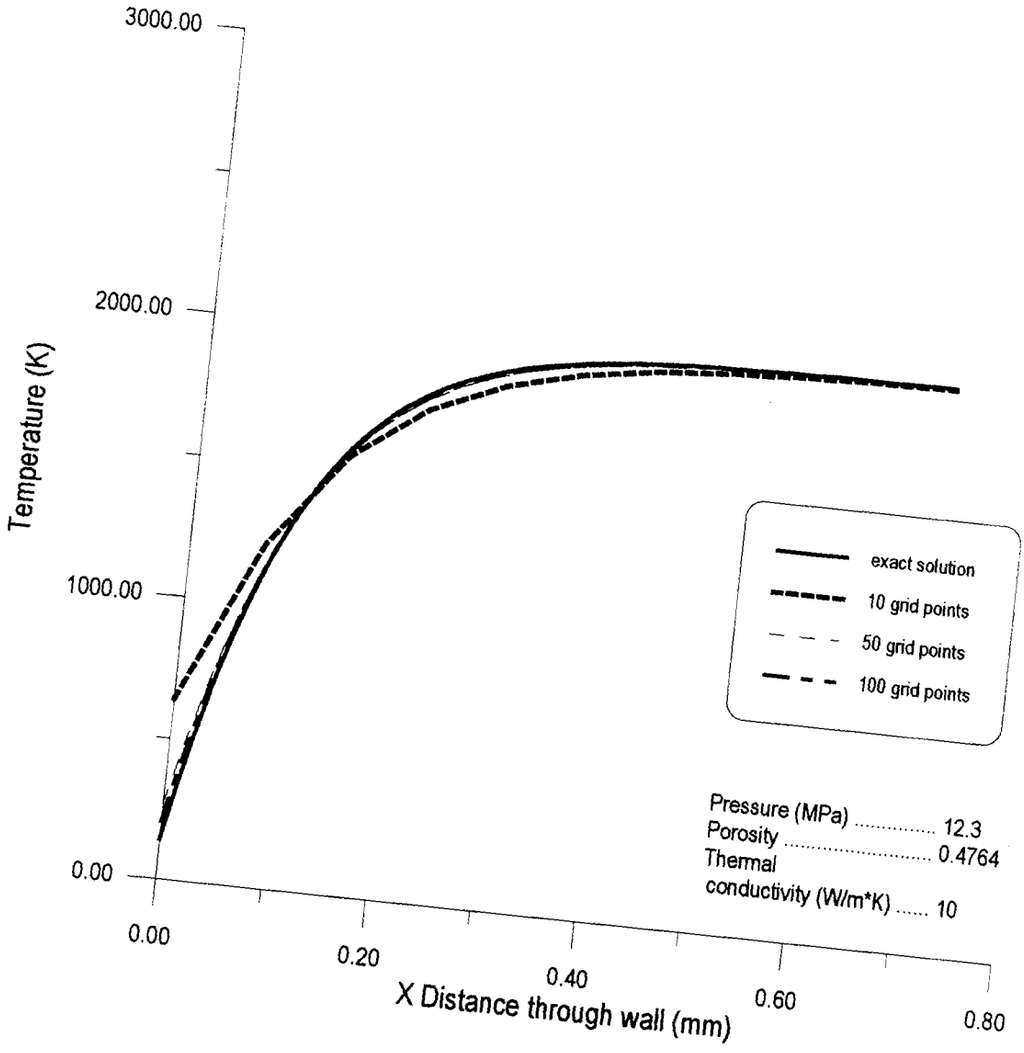

Figure 4. Grid Size Selection from TLIQUID Model

As the reader can see, the constant property TLIQUID model generated a temperature profile that matches very closely with the exact solution at a grid size of 100. Based upon these results, 100 grid points were used for the final model. The two subroutines, TSOLID and TLIQUID were then incorporated into the final model.

IV. Results

This chapter summarizes the results for the variation of parameters study. Each section addresses the varying parameter's effect on maximum wall temperature and maximum temperature gradient and compares these values to the regeneratively cooled wall case. The maximum wall temperature and maximum temperature gradient for the regeneratively cooled wall is 838.7 K and 4.26×10^5 K/m respectively. To eliminate pressure differential dependence, all trends are non-dimensionalized by using the blowing ratio of the coolant flow. The values used in this parameter study are presented below in Table 2.

TABLE 2
POROSITIES, THERMAL CONDUCTIVITIES, AND SPHERE RADII USED IN PARAMETER STUDY.

Porosity/C0	Thermal Conductivity W/(m*K)	Sphere Radius micrometers
0.1546/2.5360	0.1	10
0.3493/1.9519	1	50
0.3686/1.8940	10	100
0.4250/1.7248	100	
0.4764/1.5708	1000	

The first section addresses some general results pertaining to flow through a porous medium. The second section addresses the effects of varying thermal conductivity and blowing ratio on maximum wall temperature and maximum temperature gradient. The third section addresses the trends caused by varying solid porosity and blowing ratio. Finally the fourth section provides the effects varying porous sphere radius has upon maximum wall temperature and maximum temperature gradient.

4.1 General Result

A general result can be drawn before looking at the variation of parameters. In the past, whenever scientists have considered flow through a porous medium, they have assumed that the liquid and solid are very close to the same temperature throughout (Schneider, 1955:218). This study found this to be true for low porosity solids, but not for high porosity solids. The liquid temperature remained within 0.1% of the solid temperature profile through the entire wall thickness at a low porosity of 0.1546. This case is shown in Figure 5. Because of the low porosity, the porous wall's effective thermal conductivity is highest. With a higher thermal conductivity, the heat is conducted away from the wall surface and is distributed through the wall, thereby decreasing the maximum temperature gradient.

At higher porosities, the effective thermal conductivity is decreased. Therefore, very little heat is conducted through the solid and the cooling effect of the liquid dominates. This causes the solid and liquid to remain at essentially the same temperature throughout most of the wall. The two temperatures diverge within the last 9% of the wall thickness with a maximum difference of 39%. This effect is shown in Figure 6.

The author concludes the assumption of solid and liquid temperatures nearly the same throughout the porous wall is valid. This assumption breaks down in high porosity solids near the hot gas side boundary.

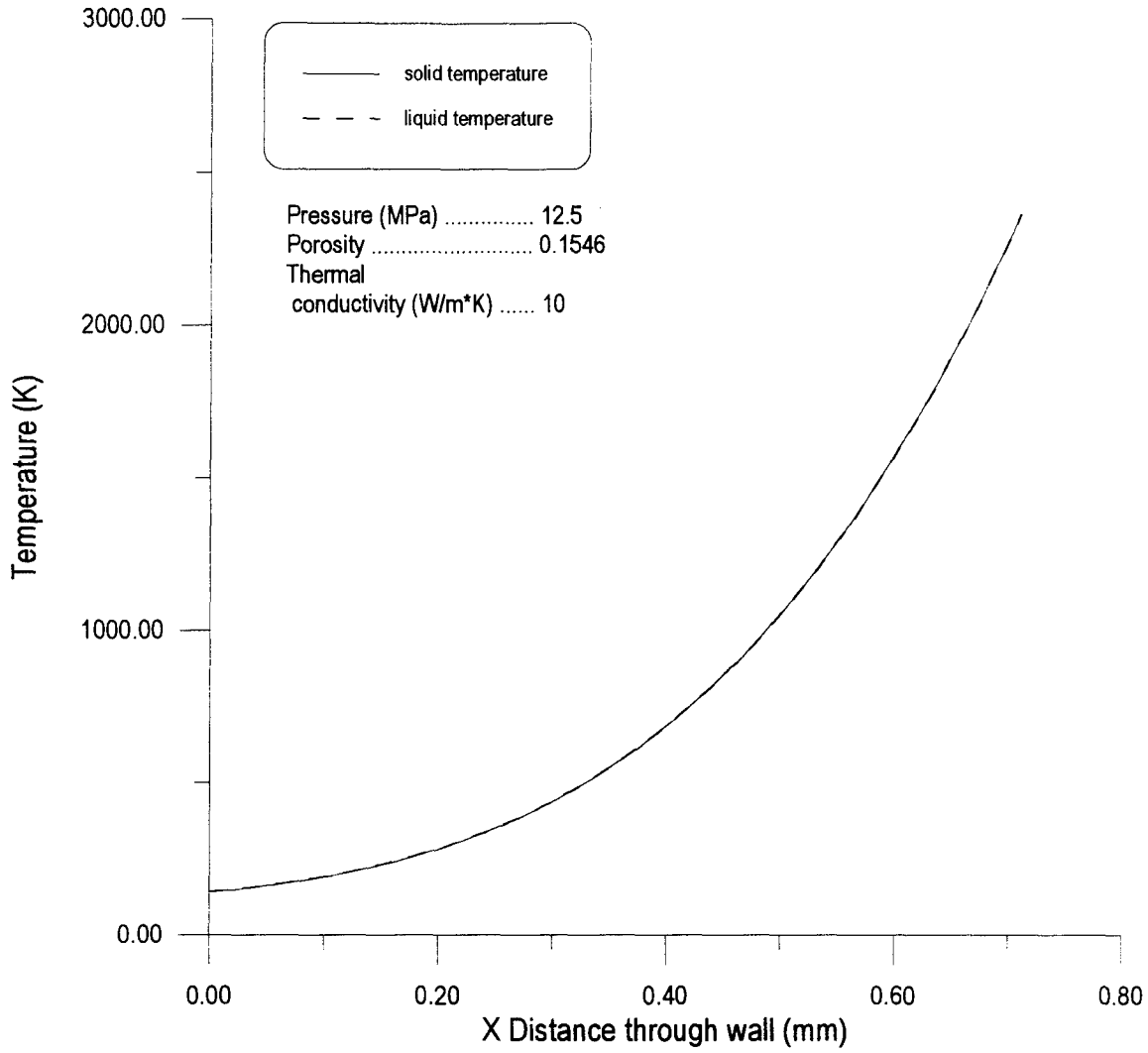

Figure 5. 0.1546 Porous Solid and Liquid Temperature Profiles

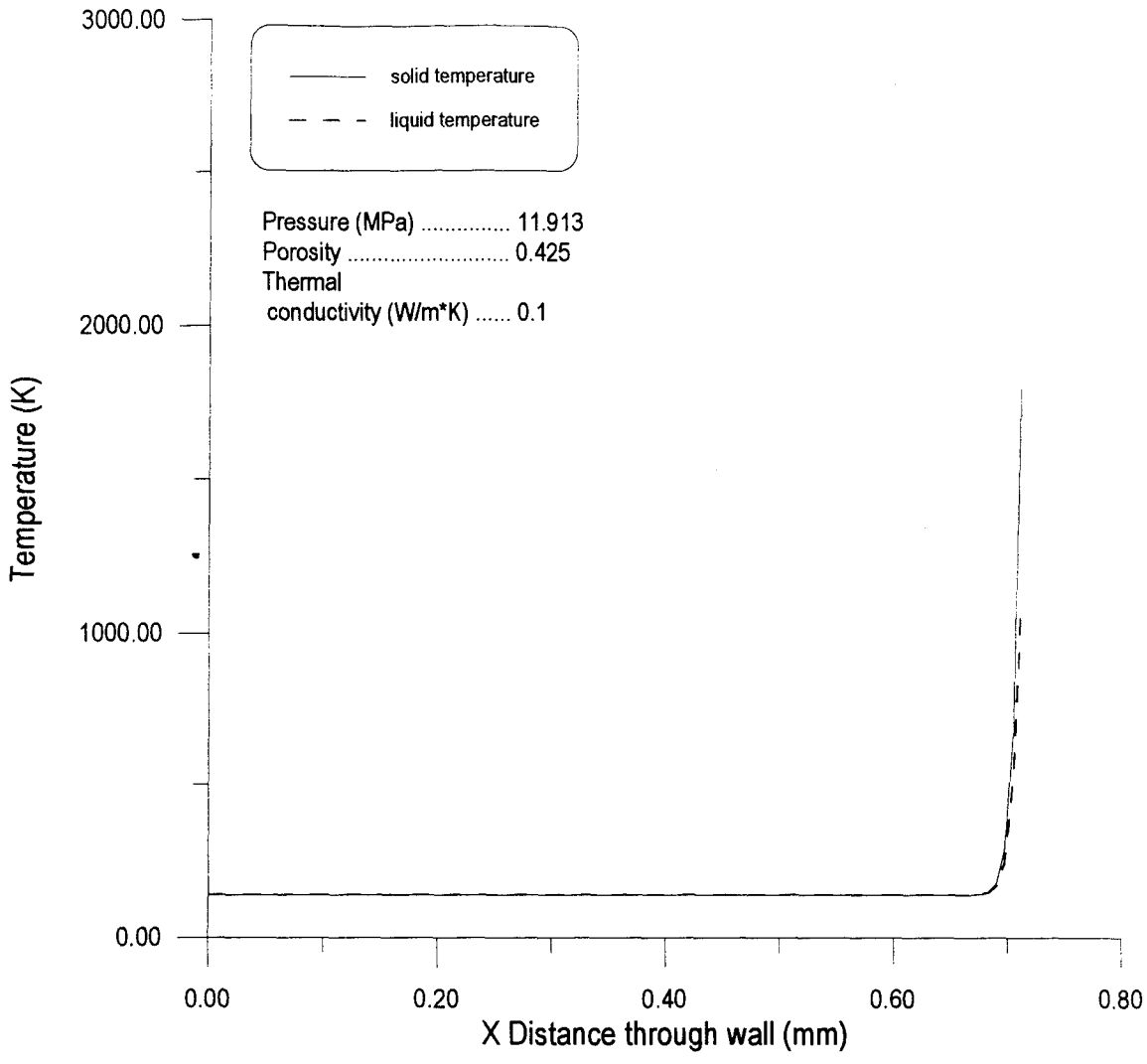

Figure 6. 0.425 Porous Solid and Liquid Temperature Profiles

4.2 Varying Solid Thermal Conductivity Results

One observation from the test data reveals that varying thermal conductivity had the greatest effect in low porosity solids. Increasing the thermal conductivity from 0.1 W/(m*K) to 1000 W/(m*K) in a solid with a porosity of 0.1546 yielded a 42% decrease in maximum wall temperature and a 95% decrease in maximum temperature gradient. The

same increase in thermal conductivity in a solid with a porosity of 0.4764 yielded only a 31% decrease in maximum wall temperature and a 72% decrease in maximum temperature gradient. The effective thermal conductivity is a very strong function of porosity. As porosity increases, the effective thermal conductivity approaches the thermal conductivity of the liquid. Therefore, at low porosities the solid thermal conductivity will dominate. At high porosities the liquid thermal conductivity will dominate. Therefore, changes in solid thermal conductivity will have a pronounced effect in low porosity solids and little effect in high porosity solids. These results are shown in Figures 7 and 8.

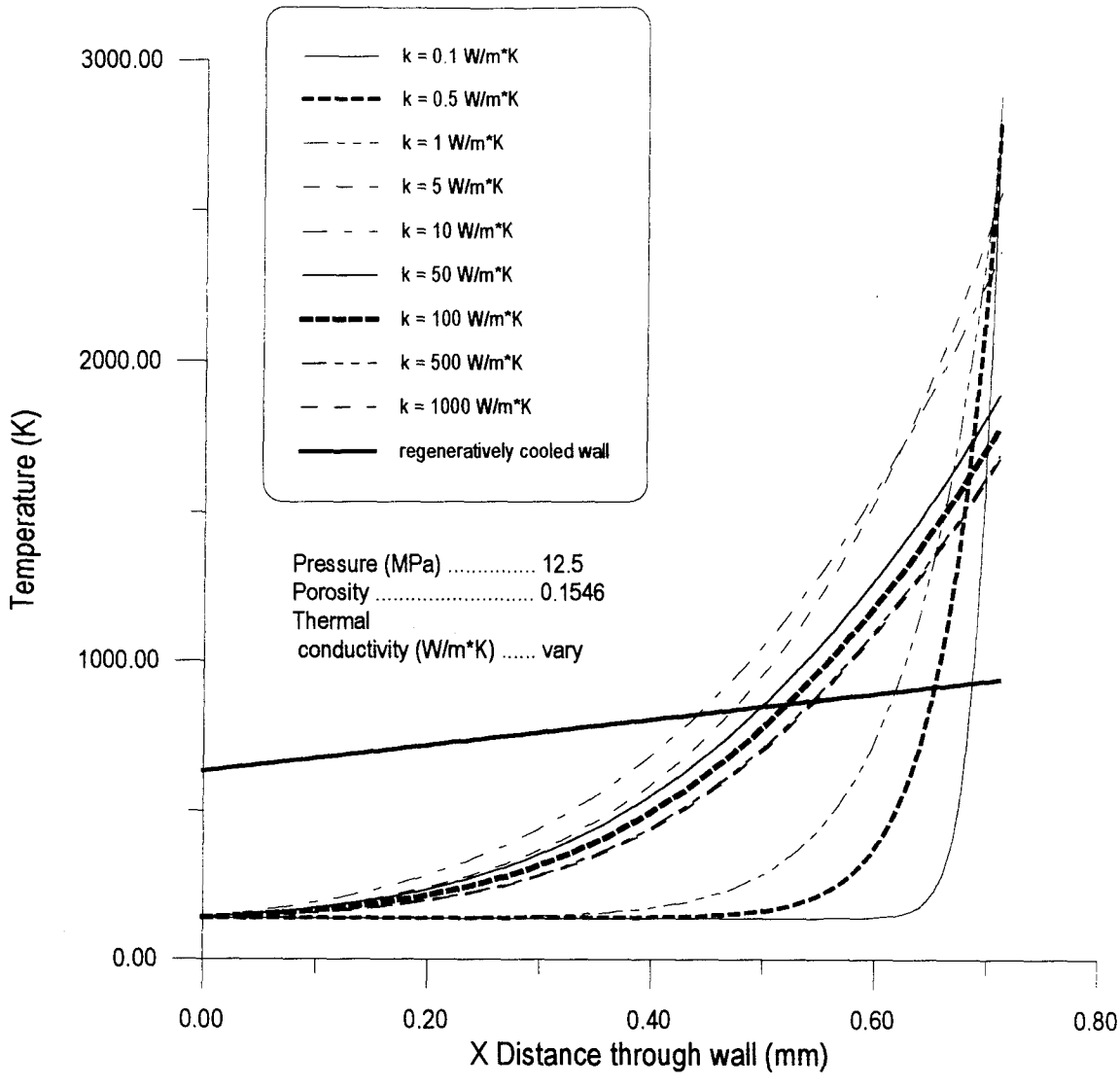

Figure 7. 0.1546 Porous Solid Temperature Profile with Varying Thermal Conductivity

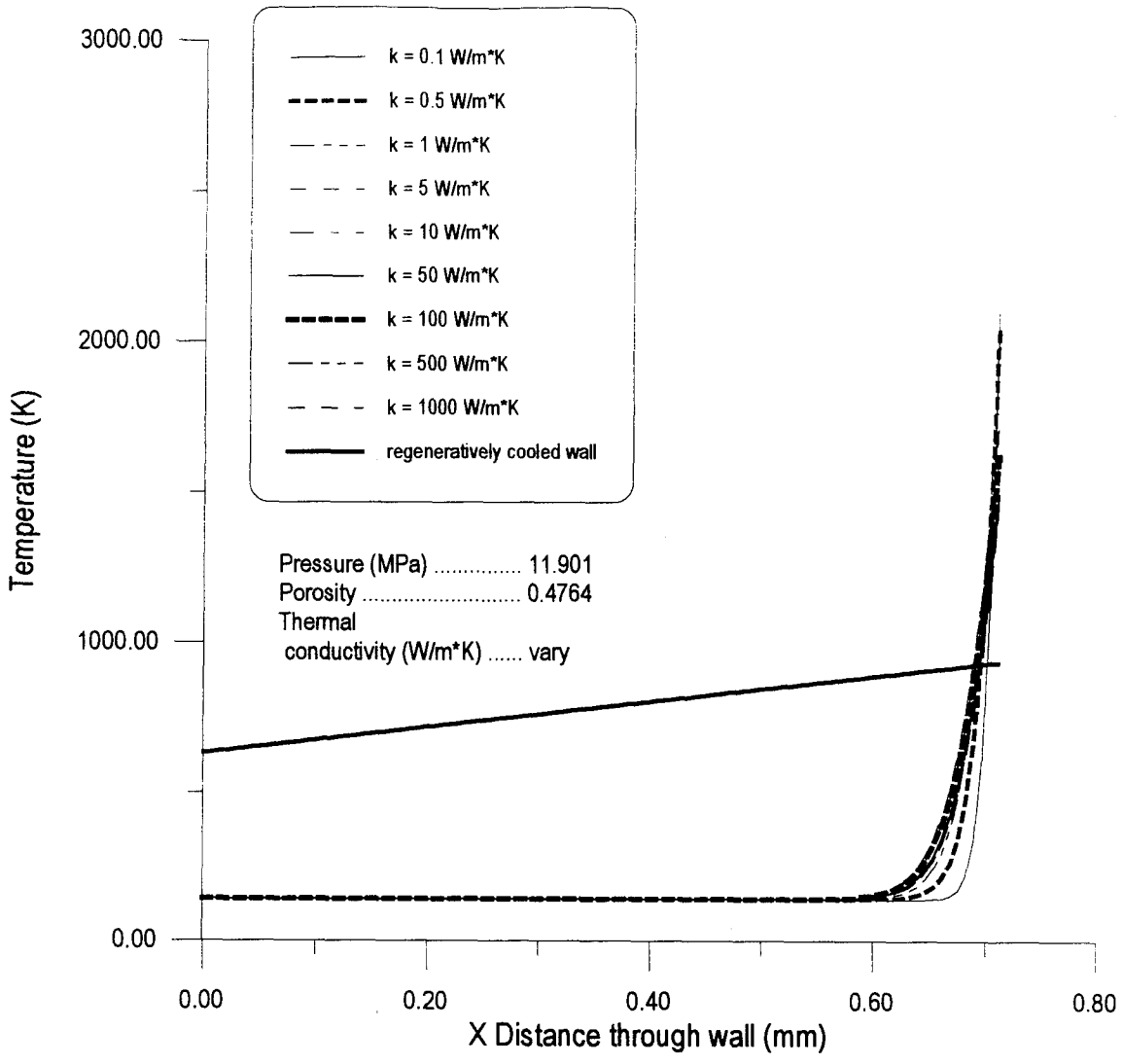

Figure 8. 0.4764 Porous Solid Temperature Profile with Varying Thermal Conductivity

The results of varying thermal conductivity in a porous solid with a porosity of 0.3493, and a sphere size of 10 micrometers, on maximum wall temperature are presented in Figure 9.

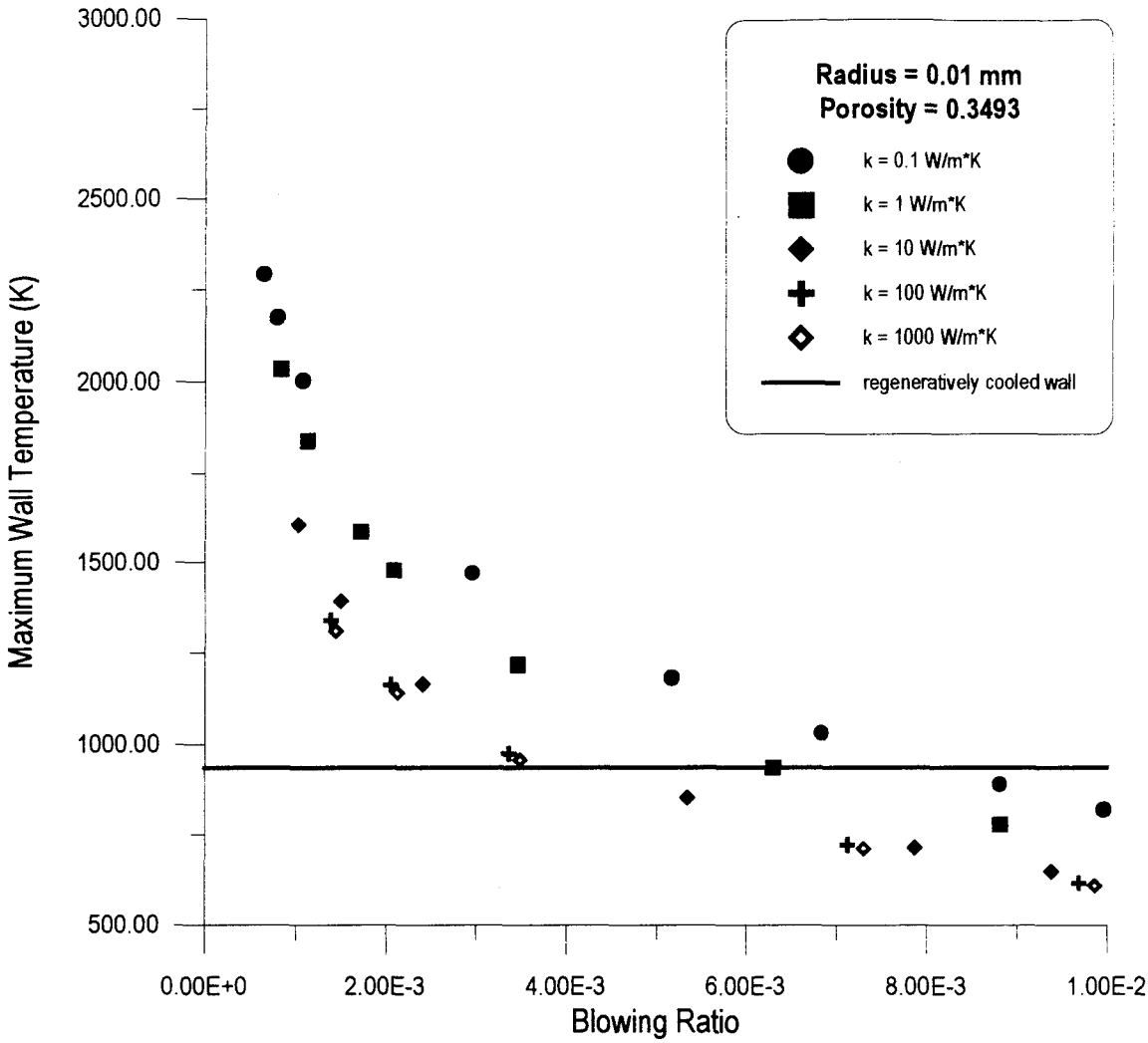

Figure 9. Varying Thermal Conductivity Effect on Maximum Wall Temperature

One observed trend was a consistent decrease in maximum wall temperature with respect to blowing ratio. For a thermal conductivity of 0.1 W/(m*K), there was a 55% decrease in maximum wall temperature as blowing ratio went from 0.06% to 0.6%. This decrease is due to two factors. One factor is the increased advection of energy by the transpiration coolant. Another is the decrease in heat flux caused by a decrease in heat

transfer coefficient. To illustrate the effect of blowing upon the maximum wall temperature, the author plotted two solid temperature profiles in Figure 10.

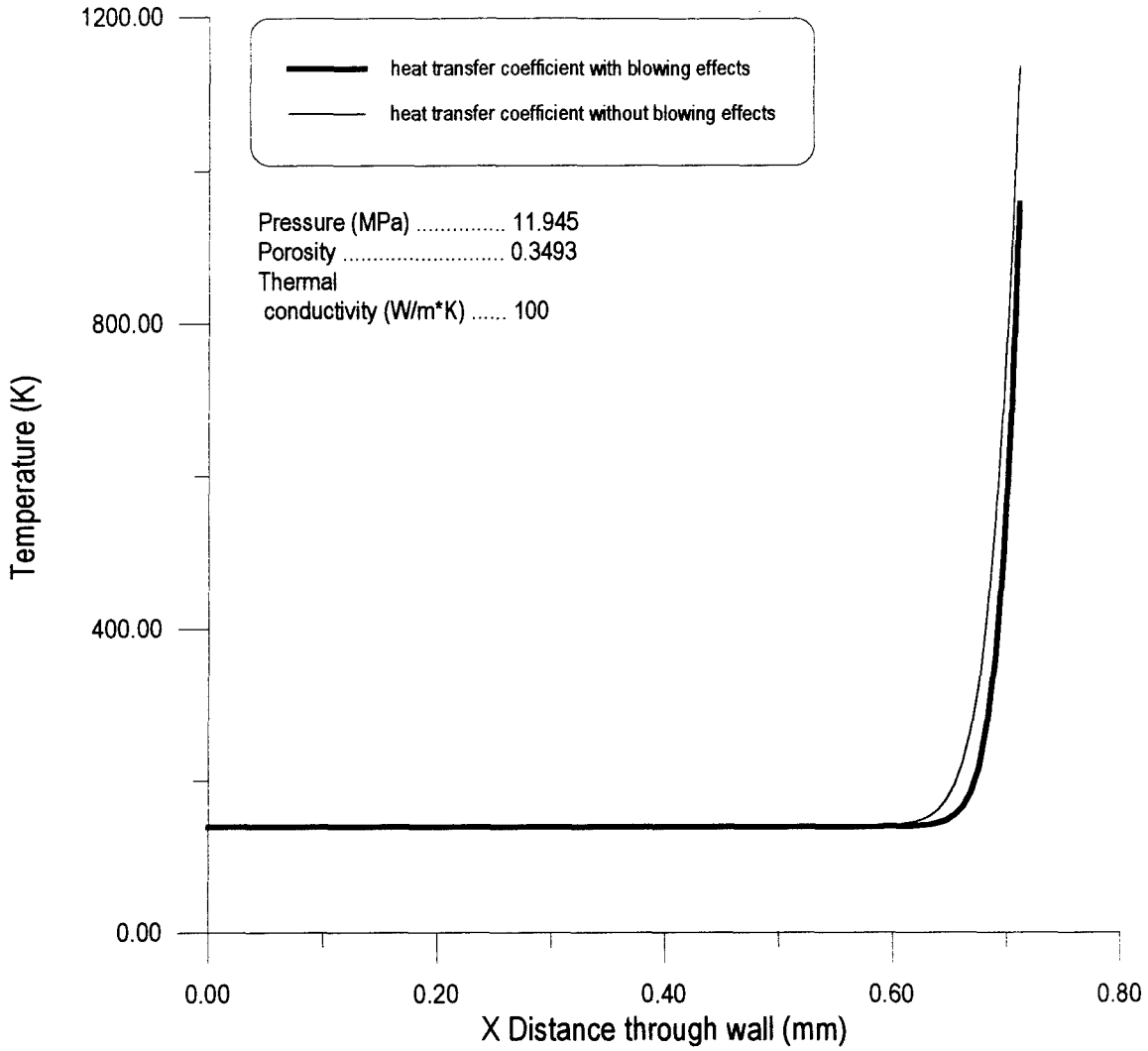

Figure 10. Blowing Effect on Liquid Temperature Profile

One profile was calculated using a heat transfer coefficient neglecting blowing effects. The other profile was calculated using Chen's correlation to include blowing effects. The blowing effect alone caused a 16% decrease in maximum wall temperature.

Another noticeable effect was the decrease in effect of blowing ratio on maximum wall temperature with increasing thermal conductivity. There was a 27% decrease in maximum wall temperature for the 1000 W/(m*K) thermal conductivity case, compared to the 55% decrease for the 0.1 W/(m*K) case. This effect is related to the increase in effective thermal conductivity.

Additionally, there is only a 6% difference in maximum wall temperatures for thermal conductivities between 10 and 1000 W/(m*K), and a 1% difference between 100 and 1000 W/(m*K) solids. Since most modern materials fall within this range of thermal conductivities, porous solids can be made of existing materials.

The transpiration cooled wall could achieve a lower maximum wall temperature than the regeneratively cooled wall at a blowing ratio as low as 0.4% for thermal conductivies between 10 and 1000 W/(m*K). At the maximum thermal conductivity and maximum blowing ratio, the transpiration cooled wall was 35% cooler than the regeneratively cooled wall. Therefore a porous wall made of existing materials with the given properties could operate at lower maximum wall temperatures than the regeneratively cooled wall.

The results of varying thermal conductivity in a porous solid with a porosity of 0.3493, and a sphere size of 10 micrometers, on maximum temperature gradient are presented in Figure 11. One observed trend was a consistent decrease in temperature gradient with increasing thermal conductivity. There was a 73% decrease in maximum temperature gradient as thermal conductivity went from 0.1 to 1000 W/(m*K). The decrease in temperature gradient is again due to the increased effective thermal

conductivity. The increased effective thermal conductivity allows the porous solid to conduct the heat further away from the hot gas surface. Unfortunately, the lowest temperature gradient achieved with transpiration cooling is still 72 times greater than the temperature gradient of regenerative cooling. A possible tradeoff would be that the decreased temperatures would allow the porous material to endure the steeper temperature gradient.

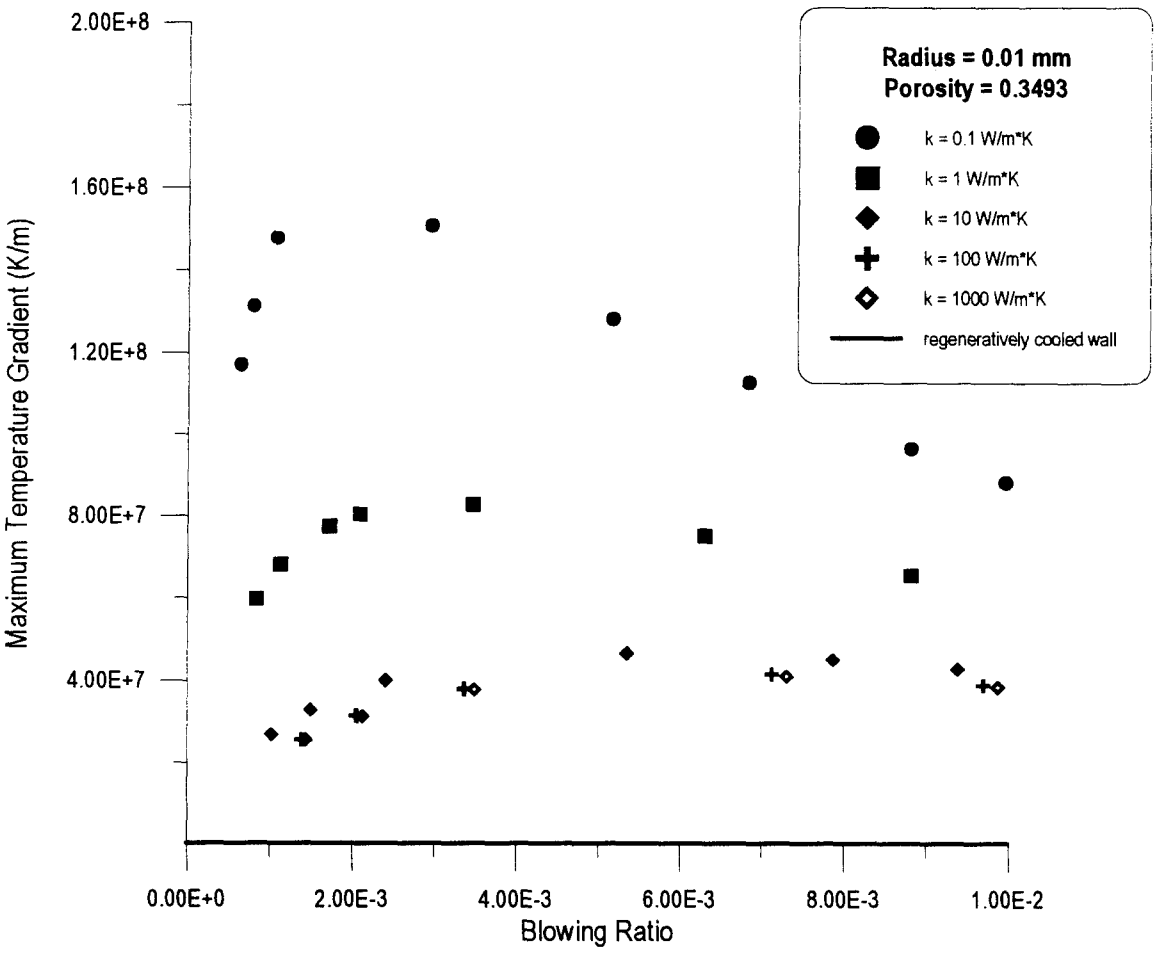

Figure 11. Varying Thermal Conductivity Effect on Maximum Temperature Gradient

Another trend was an increase in maximum temperature gradient at low blowing ratios and a decrease in maximum temperature gradient at high blowing ratios. This effect is possibly due to two competing factors. As mentioned earlier, as blowing ratio increases, the hot gas side heat transfer coefficient decreases. This would cause a decrease in temperature gradient. But an increase in blowing ratio causes the majority of the heat transfer between the solid and liquid to take place closer to the hot gas surface thereby increasing the temperature gradient. Since existing materials fall in the mid to high thermal conductivity range where these temperature gradient effects are less pronounced, this trend is not important

From these results, the optimum porous material would be made of the highest thermal conductivity. The material would also operate at the highest blowing ratio to obtain the lowest maximum wall temperature.

4.3 Varying Solid Porosity Results

The results of varying porosity in a porous solid with a thermal conductivity of 100 W/(m*K), and a sphere size of 10 micrometers, on maximum wall temperature are presented in Figure 12.

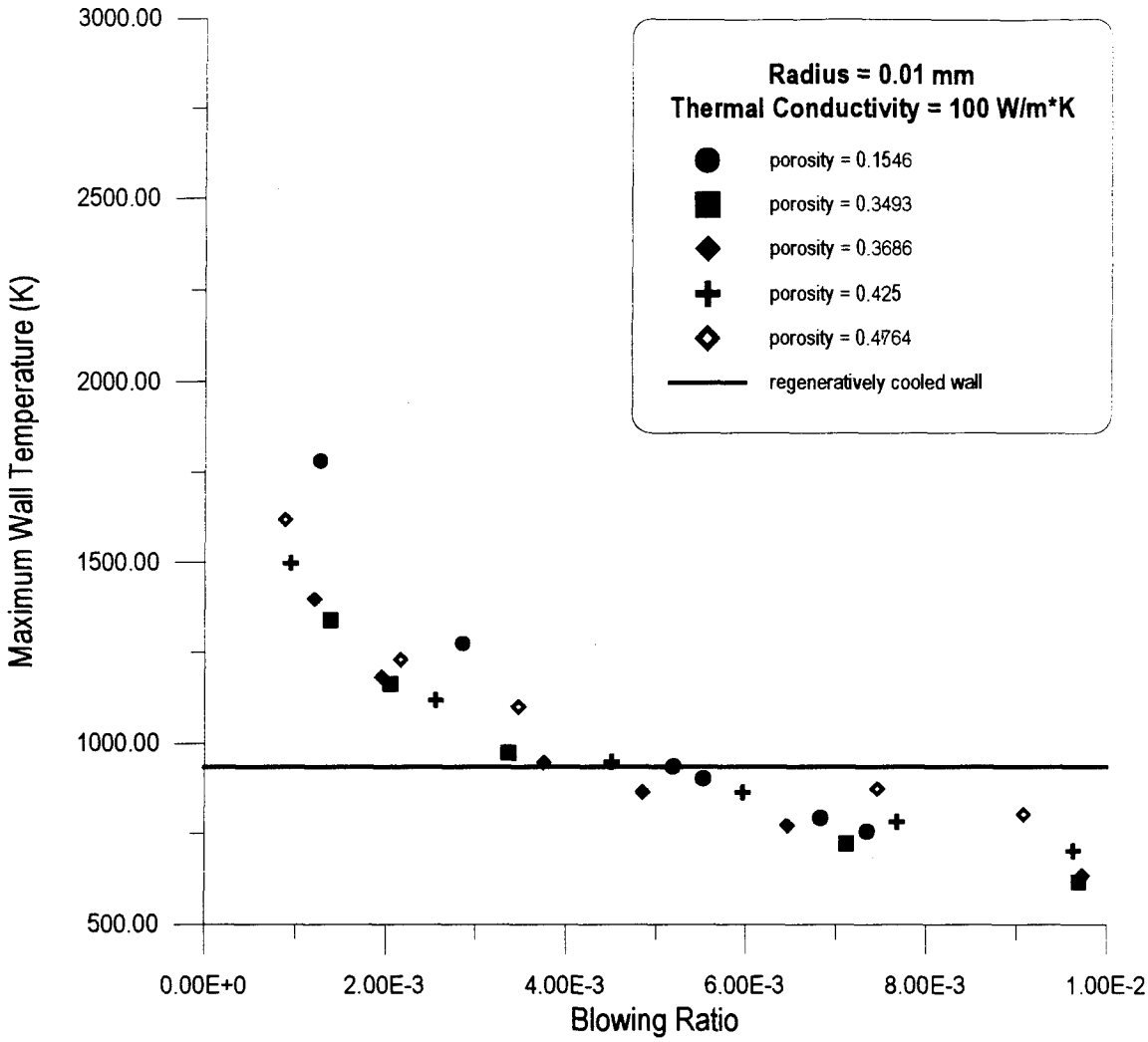

Figure 12. Varying Porosity Effect on Maximum Wall Temperature

A trend observed in the previous section was that increasing porosity affected the effective thermal conductivity of the porous solid. Following this reasoning, it would appear that the porous material with the lowest porosity and highest thermal conductivity would have the lowest maximum wall temperature. But as the reader can see in Figure 12, maximum wall temperature decreases with increasing porosity, then increases again. The minimum

wall temperature occurs near a porosity of 0.3493. Apparently there is an inflection point where the increased coolant available for energy absorption at larger porosities is offset by decreased effective thermal conductivity and decreased porous solid surface area. As porosity increases, the surface area exposed to flow decreases. The optimum case seems to be where the porosity is large enough to allow a large mass transfer of coolant, but not large enough to diminish the effective thermal conductivity. The porous solid with a porosity of 0.3493 operates at a 15% lower temperature than the 0.1546 solid and at a 23% lower temperature than the 0.4764 solid.

The results of varying porosity in a porous solid with a thermal conductivity of 100 W/(m*K), and a sphere size of 10 micrometers, on maximum temperature gradient are presented in Figure 13. As porosity increases, the maximum temperature gradient increases. Since the effective thermal conductivity decreases with increasing porosity, the amount of heat conducted into the porous solid decreases. Therefore all the heat transfer between the transpiration coolant and the solid has to occur near the hot gas side wall. Therefore the temperature gradients have to increase because the temperature change has to occur over a shorter and shorter distance. The temperature gradient increased over 27 times as porosity increased from 0.1546 to 0.4764.

From these results, if only maximum wall temperature is considered, the optimum porous material would be made with a porosity of approximately 0.3493. The design engineer would have to consider the effect of increased temperature gradients due to the higher porosity.

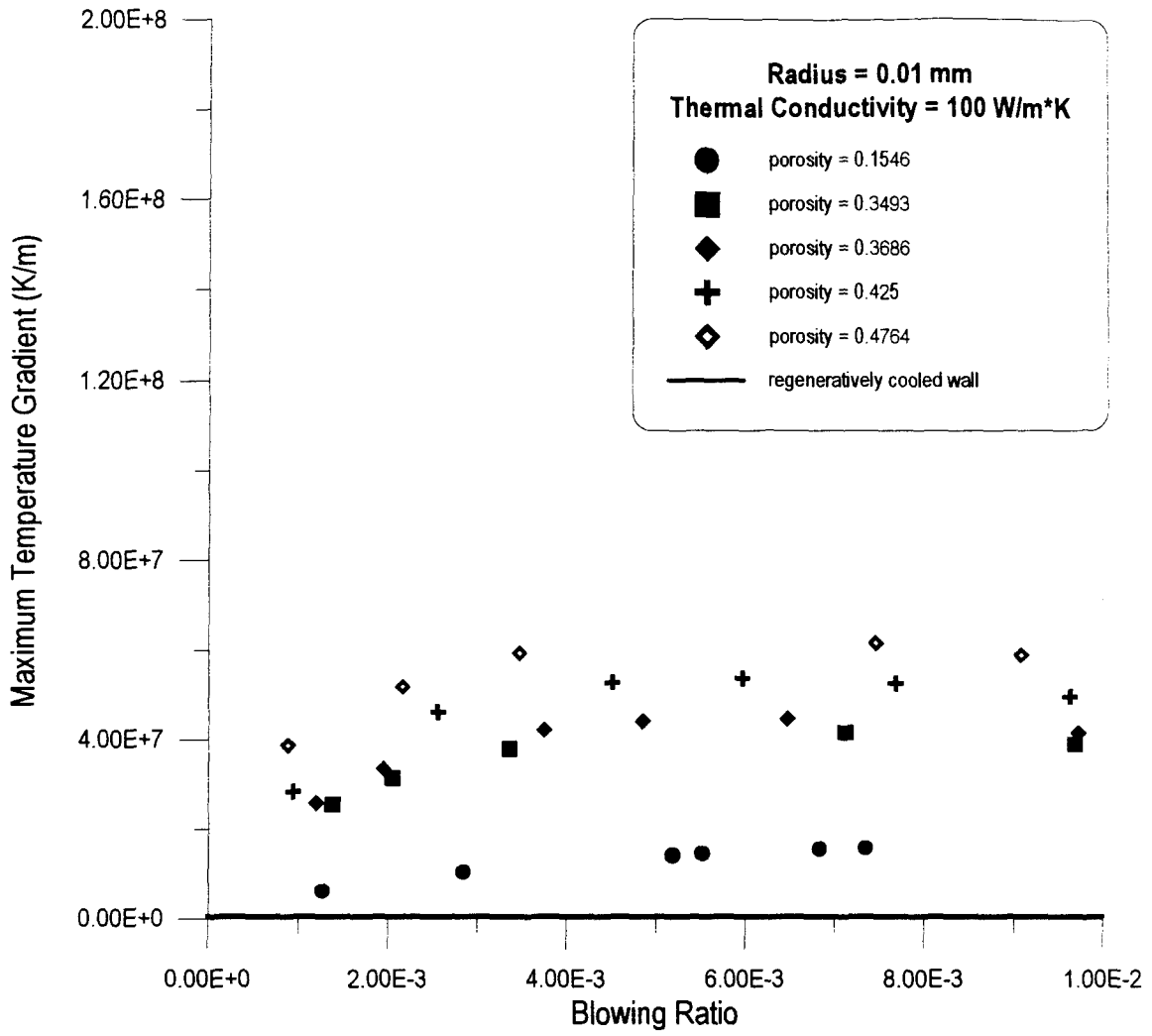

Figure 13. Varying Porosity Effect on Maximum Temperature Gradient

4.4 Varying Porous Sphere Radius Results

The porous material sphere sizes used were limited due to the wall thickness. Because the wall is only 711.2 micrometers thick, spheres larger than 200 micrometers in diameter were not considered. The results of varying sphere size in a porous solid with a

porosity of 0.3493, and a thermal conductivity of 100 W/(m*K), on maximum wall temperature are presented in Figure 14.

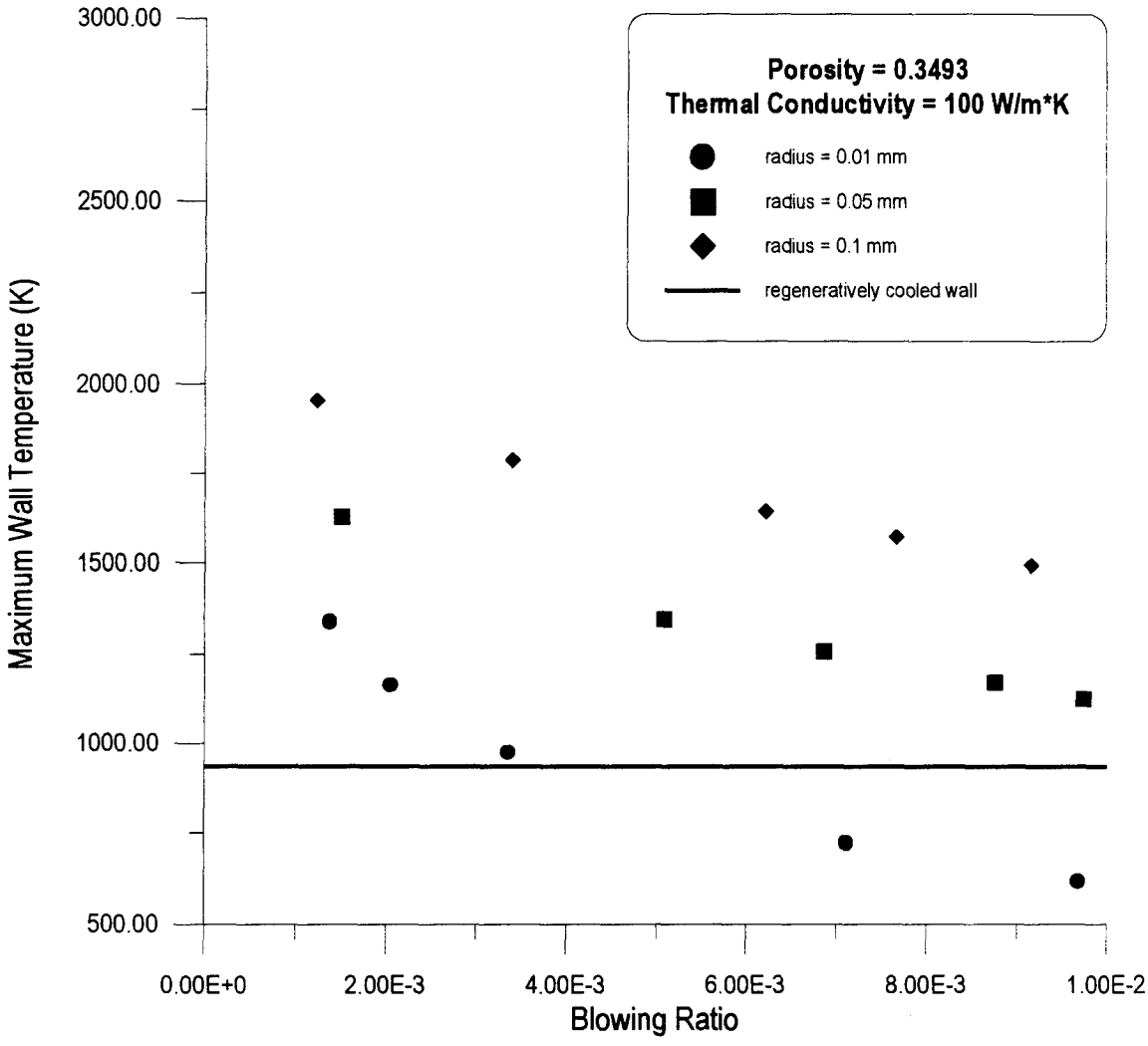

Figure 14. Varying Porous Sphere Radius Effect on Maximum Wall Temperature

There was a 142% increase in maximum wall temperature by increasing the sphere radius from 10 micrometers to 100 micrometers. This effect is due to the drastically reduced

surface area exposed to the transpiration coolant flow. Since the surface area exposed to the coolant flow takes the form

$$A^* = C0\left(\frac{x}{r_p}\right)A \tag{27}$$

where A^* is the solid surface area exposed to the flow, $C0$ is a proportionality constant defined by the geometrical arrangement of the spherical particles, x is the distance through the wall, r_p is the spherical particle radius, and A is the transpiration coolant flow cross-sectional area. From this equation, A^* increases as r_p decreases. Therefore, the most heat transfer from the solid to the transpiration coolant occurs with the smallest radius spheres.

The results of varying sphere size in a porous solid with a porosity of 0.3493, and a thermal conductivity of 100 W/(m*K), on maximum temperature gradient are presented in Figure 15.

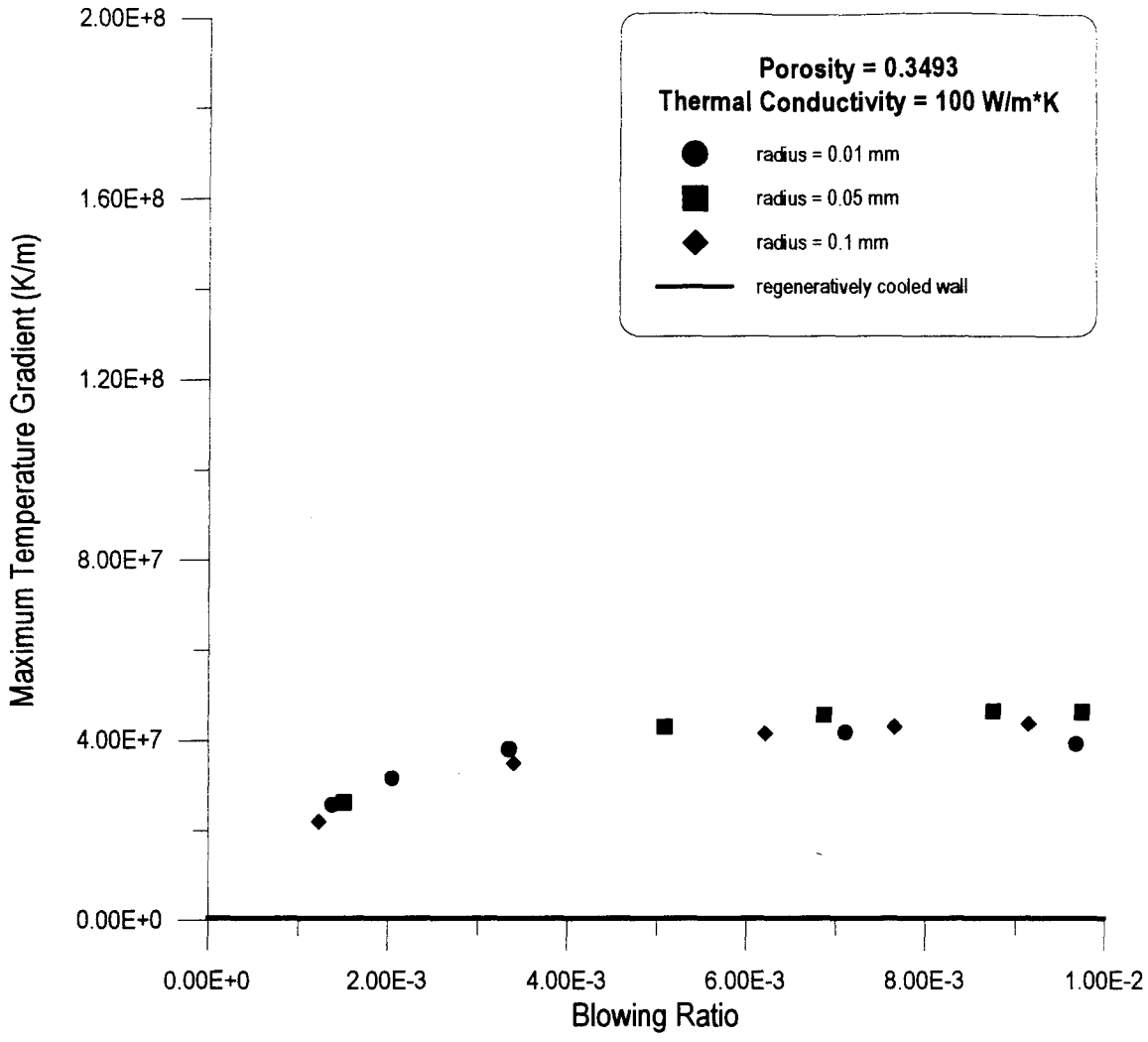

Figure 15. Varying Porous Sphere Radius Effect on Maximum Temperature Gradient

Maximum temperature gradient varied less than 10% across the entire range of blowing ratios. Therefore, there was little to no effect of varying porous sphere radius on temperature gradient. From these results, the optimum porous material would be made of the smallest diameter spheres possible without impeding coolant flow.

V. Conclusions and Recommendations

5.1 Conclusions

The author created a numerical model to compare the effect of porosity, thermal conductivity, and blowing ratio upon the solid temperature profile within a porous, transpiration cooled rocket nozzle. The maximum wall temperature and maximum temperature gradient for each case was compared to the maximum wall temperature and maximum temperature gradient for the regeneratively cooled wall case. The transpiration cooled wall could achieve lower maximum wall temperatures than the regeneratively cooled wall with blowing ratios as low as 0.4%. The transpiration cooled wall could operate at a maximum 35% colder than the regeneratively cooled wall. Unfortunately, transpiration cooling results in a temperature gradient that is 72 times steeper than the regeneratively cooled wall. Therefore, the material chosen for the porous wall must be able to withstand extreme temperature gradients. The maximum temperature gradient is located at the hot gas surface of the porous wall. The optimum configuration for the cases studied would be a medium (0.3493) porosity, high (1000 W/(m*K)) thermal conductivity, and high (1%) blowing ratio transpiration cooled nozzle. The thermal conductivity and blowing ratio values represent the largest values tested in this study. Since the medium thermal conductivity results were not substantially different from the high thermal conductivity results, existing materials (100 - 500 W/m*K thermal conductivities) could be used to make the porous nozzle wall.

5.2 Recommendations

The author hopes that this study will shed some new light on the feasibility of using transpiration cooling as a method for cooling the throat region of long operating duration, liquid-fueled rocket nozzles. One recommendation is to build upon the model shown in this study and tailor it to other specific problems. Modifications could include increasing the accuracy of the liquid initial boundary condition by solving the turbulent boundary layer problem to obtain the two coolant temperature values prior to contact with the porous solid. Another recommedation would be to choose more accurate heat transfer correlations for the boundary conditions. This thesis test case using the SSME MCC is specifically narrow. The blowing ratios used were small, and geometric and thermodynamic conditions were tailored for the SSME MCC case. The author recommends that future research could use the basic outline of this model to test against experimental transpiration cooled thrust chambers.

Appendix A. Derivation of Energy Equations

This appendix presents the derivation of the energy equations used to calculate the solid and liquid temperature profiles and their conversion to the finite difference forms. The first section addresses the solid energy equation. The second section covers the liquid energy equation. The third and fourth sections address the finite difference forms of the solid and liquid energy equations respectively.

A.1 Solid Energy Equation

The derivation begins by performing an energy balance on a differential control volume of the porous solid material. The energy balance takes the form

$$\dot{E}_{in} + \dot{E}_{generated} - \dot{E}_{out} = \dot{E}_{stored} \tag{A1}$$

where $\dot{E}_{in}$ is the rate of energy entering the control volume, $\dot{E}_{generated}$ is the rate of energy generated within the control volume, $\dot{E}_{out}$ is the rate of energy leaving the control volume, and $\dot{E}_{stored}$ is the rate of energy stored within the control volume (Incropera and DeWitt, 1990:15). This study only considers heat transfer in one dimension represented by x, with no heat generation within the solid. The energy processes within the porous solid are represented below in Figure A1.

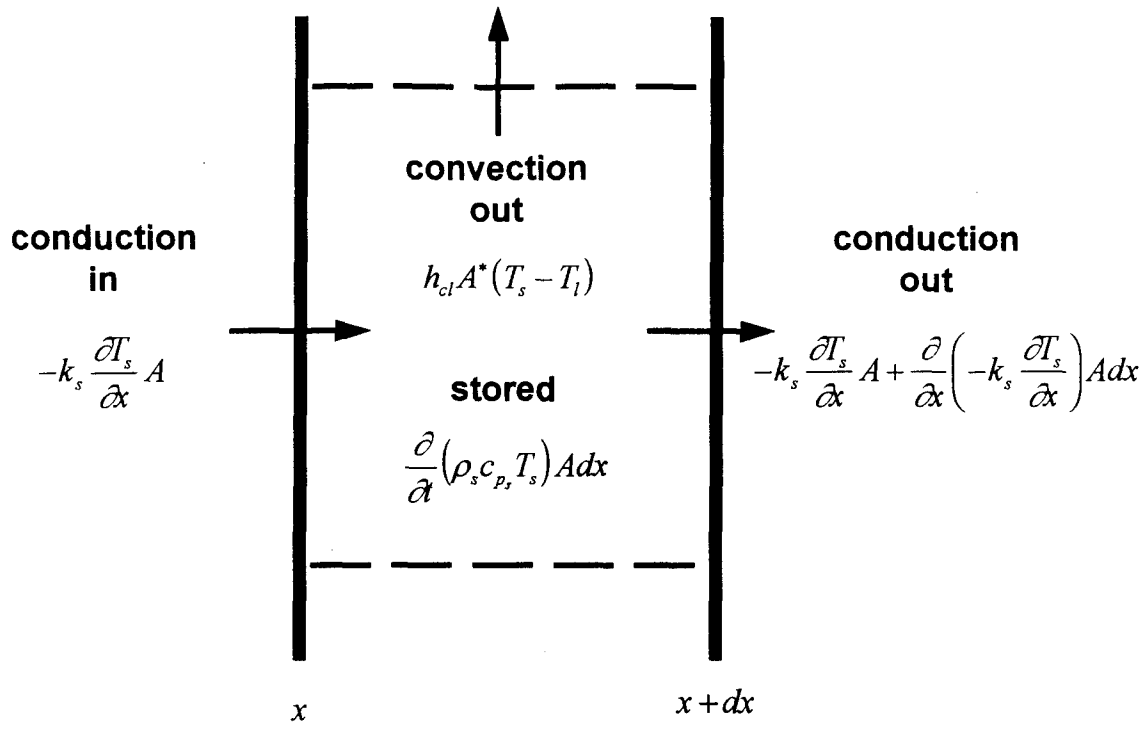

Figure A1. Energy Balance on a Solid Differential Control Volume

Representing the energy processes in equation form below yields the equation below.

$$-k_s \frac{\partial T_s}{\partial x} A - \left[-k_s \frac{\partial T_s}{\partial x} A + \frac{\partial}{\partial x}\left(-k_s \frac{\partial T_s}{\partial x}\right) A dx \right] - h_{cl} A^* (T_s - T_l) = \frac{\partial}{\partial t}(\rho_s c_{p_s} T_s) A dx \quad \text{(A2)}$$

where k_s is the effective thermal conductivity of the porous solid wall, $\frac{\partial T_s}{\partial x}$ is the temperature gradient through the porous solid wall, A is the conduction cross sectional area, dx is the differential distance in the x direction, h_{cl} is the heat transfer coefficient between the porous solid and the transpiration coolant, A^* is the surface area of the

porous solid exposed to transpiration coolant flow, and $\frac{\partial}{\partial t}\left(\rho_s c_{p_s} T_s\right) A dx$ represents the transient temperature effects within the porous solid.

Since the energy transfer is one dimensional in space and time, all partial differentials become total derivatives. Also, since the effective thermal conductivity takes into account the porosity of the solid material, the conduction cross sectional area used becomes the total area, A, not the $(1-\varepsilon)A$ area as previous analyses have assumed (Schneider, 1955:219). Assuming constant properties with respect to the x direction and time, canceling like terms, and dividing by Adx yields the final form of the solid energy equation shown below.

$$k_s \frac{d^2 T_s}{dx^2} - \frac{h_{cl} A^* \left(T_s - T_l\right)}{Adx} = \rho_s c_{p_s} \frac{dT_s}{dt} \tag{A3}$$

A.2 Liquid Energy Equation

The derivation of the liquid energy equation also begins with an energy balance on a differential control volume in the x direction. The liquid energy equation assumes there is no heat generation within the liquid and that the liquid behaves like an ideal gas. The energy processes that take place within the liquid inside the porous solid are represented in Figure A2.

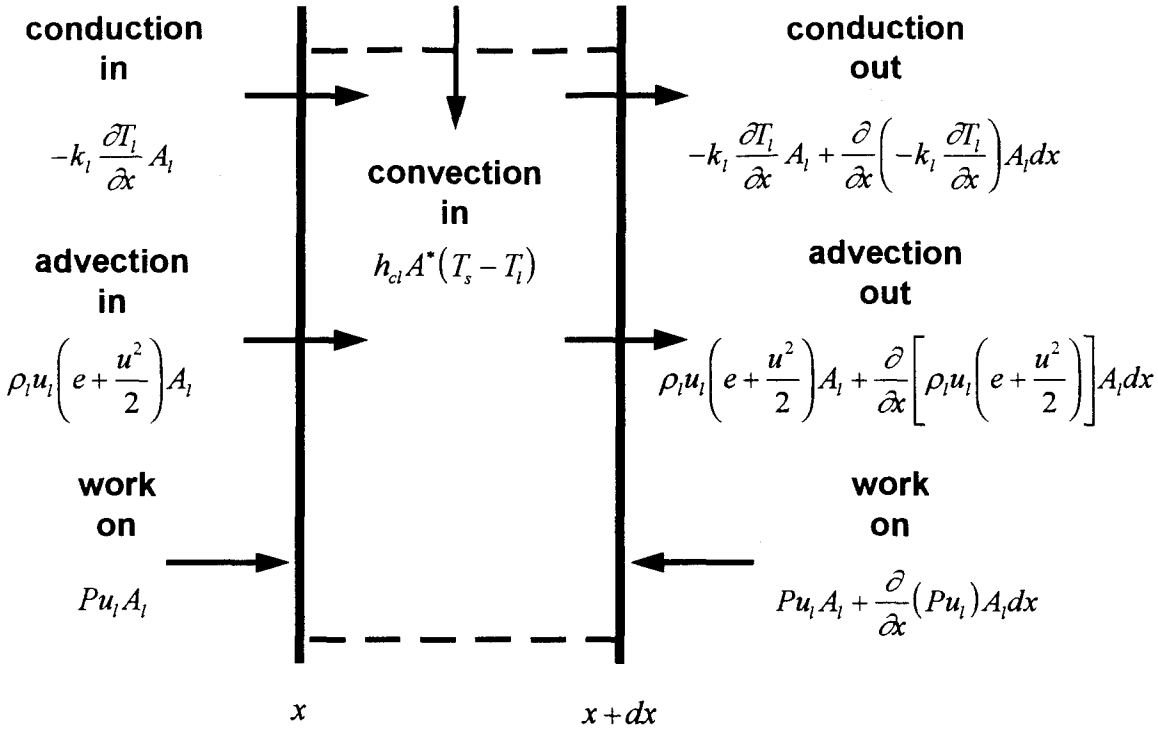

Figure A2. Energy Balance on a Liquid Differential Control Volume

This energy balance assumes that the only work done on the fluid is by pressure forces and body forces are negligible. The area used in these equations is the liquid cross sectional area defined by the porosity $A_l = \varepsilon A$. The advection term represents the internal and kinetic energy of the fluid flow crossing the control volume. A more convenient form uses enthalpy rather than internal energy. Enthalpy is defined as

$$i = e + \frac{P}{\rho_l} \tag{A4}$$

where i is the enthalpy of the fluid, e is the internal energy of the fluid, P is the pressure on the fluid, and ρ_l is the density of the fluid (Incropera and DeWitt, 1990:334). Combining terms from all the energy processes, assuming steady state, assuming the coolant is an ideal gas, assuming the $\rho_l \frac{u_l^3}{2}$ term is small compared to the temperature gradient within the fluid, and further simplifying yields the final form of the energy equation shown below.

$$k_l \frac{d^2 T_l}{dx^2} + \frac{h_{cl} A^* (T_s - T_l)}{A_l dx} - \rho_l u_l c_{p_l} \frac{dT_l}{dx} = 0 \qquad \text{(A5)}$$

A.3 Finite Difference Form of the Solid Energy Equation

This study employed an explicit finite differencing technique to solve the solid differential energy equation for the solid temperature profile. Dividing the porous wall into N regions means that there has to be N+1 grid points. The first grid point represents the conditions on the cold gas side of the wall. Consequently, the N+1 grid point represents the hot gas side conditions. At each grid point, the differential equation requires initial conditions in space and time. Because the problem is second order in space and first order in time, the problem requires two initial conditions in space and one initial condition in time. The general form of the finite difference form is given below in Equation A6.

$$k_s \frac{\left[T_s^{old}(N+1) + T_s^{old}(N-1) - 2T_s^{old}(N)\right]}{dx^2} - \frac{h_{cl}^{old} A^* [T_s^{old}(N) - T_l^{old}(N)]}{A dx} = \rho_s c_{p_s} \frac{[T_s^{new}(N) - T_s^{old}(N)]}{dt} \qquad \text{(A6)}$$

where the $(N+1)$, $(N-1)$, and (N) terms refer to the grid point being used for the calculation, and the *old* and *new* superscripts refer to the time dependence of the equation (Anderson and others, 1984:333). The reader can see that the equation can be solved for $T_s^{new}(N)$ directly as long as the old temperatures at the $(N+1)$, $(N-1)$, and (N) are known. This equation has to be modified at the first and last grid points because there is not two sided conduction taking place. The boundary conditions at these locations are governed by the heat flux between the porous solid and the hot combustion gases and the cold convective coolant respectively. The TSOLID subroutine begins with an initial temperature distribution at time equals zero. The subroutine selects a time step, dt, based upon the grid size and stability criteria, and marches forward through the porous wall in both space and time until the temperature does not change beyond a threshold value. Once this tolerance is reached, the solid has reached its steady state temperature profile.

A.4 Finite Difference Form of the Liquid Energy Equation

Unfortunately, the liquid solution is a bit more complicated. Unlike the solid energy equation, the second spatial initial condition is not known at the last grid point. Fortunately, two coolant temperatures are known just before entering the porous solid. This study assumes these temperatures to be the bulk fluid temperature of the coolant within the coolant channel. More accurate values could be found by calculating the boundary layer temperature profile within the coolant channel. For the purposes of this study, the bulk temperature of the fluid was sufficient. The finite difference form of the liquid energy equation takes a slightly modified form from the solid energy equation.

$$k_l \frac{[T_l^{new}(M-2)+T_l^{new}(M)-2T_l^{new}(M-1)]}{dx^2}+\frac{h_{cl}A^*[T_s^{old}(N)-T_l^{new}(M)]}{A_l dx} \qquad \text{(A7)}$$
$$-\rho_l u_l c_{p_l}\frac{[T_l^{new}(M)-T_l^{new}(M-1)]}{dx}=0$$

where the liquid values are calculated along M points. N and M are related by M=N+2. Therefore, at the first solid grid point N=1, the liquid temperature profile is M=3. This equation can be solved directly for $T_l^{new}(M)$ since the values of $T_l^{new}(M-2)$ and $T_l^{new}(M-1)$ are known at all times. The TLIQUID subroutine takes an initial solid temperature profile and the two known grid points, $T_l^{new}(1)$ and $T_l^{new}(2)$, and marches forward through the porous solid until it reaches the last grid point. Like the TSOLID subroutine, the TLIQUID subroutine compares the new liquid temperature profile to the previous profile and watches for the difference to be within a specified tolerance. The liquid has reached its steady state temperature profile once this tolerance is reached.

Appendix B. Thesis Computer Code

Attached is the final computer code in FORTRAN used to compute the temperature profiles for the porous solid and liquid transpiration coolant.

```
      PROGRAM THESIS
C
C  THIS PROGRAM CALCULATES THE TEMPERATURE PROFILES
C  FOR A POROUS SOLID AND THE LIQUID TRANSPIRATION
C  COOLANT OF A ROCKET NOZZLE WITH THE SPACE SHUTTLE
C  MAIN ENGINE MAIN COMBUSTION CHAMBER COMBUSTION PRODUCTS,
C  HYDROGEN COOLANT, AND NOZZLE GEOMETRY
C
      IMPLICIT NONE
C
C  VARIABLES USED IN MAIN PROGRAM
C
C     TSOLD = VECTOR OF POROUS SOLID TEMPERATURE AT PREVIOUS TIME STEP
C     TLOLD = VECTOR OF TRANSPIRATION COOLANT TEMPERATURE AT PREVIOUS
C           TIME STEP
C     TSNEW = SOLID TEMPERATURE AT NEW TIME STEP
C     TLNEW = COOLANT TEMPERATURE AT NEW TIME STEP
C     DX = X DISTANCE STEP SIZE THROUGH WALL
C     RHOLAVG = AVERAGE COOLANT DENSITY
C     MULAVG = AVERAGE COOLANT VISCOSITY
C     DIFF = TOLERANCE USED TO DETERMINE CONVERGENCE
C     DELTAS = SUM OF THE SQUARES DIFFERENCE OF SOLID TEMPERATURES
C     DELTAL = SUM OF THE SQUARES DIFFERENCE OF COOLANT TEMPERATURES
C     KL = LOCAL COOLANT THERMAL CONDUCTIVITY
C     DIFFLIM = SPECIFIED TOLERANCE USED TO DETERMINE CONVERGENCE
C     N = INDEX USED FOR SOLID TEMPERATURE ARRAY
C     M = INDEX USED FOR COOLANT TEMPERATURE ARRAY
C     LASTX = GRID SIZE
C     STEP = COUNTER THAT INDICATES NUMBER OF ITERATIONS OF MAIN LOOP
C
C  DECLARE THE VARIABLES
C
      DOUBLE PRECISION TSOLD, TLOLD, TSNEW, TLNEW, DX
      DOUBLE PRECISION RHOLAVG, MULAVG, DIFF
      DOUBLE PRECISION DELTAS, DELTAL, KL, DIFFLIM

      INTEGER N, M, LASTX, STEP
C
C  DIMENSION THE VARIABLES THAT ARE ARRAYS
C
      DIMENSION TSOLD(20000), TLOLD(20000), TSNEW(20000), TLNEW(20000)
      DIMENSION KL(20000)
C
C  THIS COMMON BLOCK CONTAINS THE GRID DIMENSIONS USED
C
      COMMON /DIMEN/ LASTX, DX
C
C  BEGIN THE PROGRAM BY SPECIFYING THE INITIAL CONDITIONS
C
      CALL INPUT(TSOLD, TLOLD, RHOLAVG, MULAVG, DIFFLIM, TLNEW)
```

```
C
C  INITIALIZE THE CONVERGENCE CRITERIA VARIABLE, DIFF, TO A VERY
C  LARGE NUMBER TO BEGIN MAIN LOOP
C
      DIFF = 9999.0
      STEP = 0
C
C  BEGIN THE MAIN LOOP AND CONTINUE TO ITERATE UNTIL THE SUM OF
C  THE SQUARES OF THE SOLID AND COOLANT TEMPERATURES IS LESS THAN
C  THE SPECIFIED TOLERANCE, DIFFLIM
C
      DO WHILE (DIFF.GE.(DIFFLIM))
C
C  CALCULATE A NEW COOLANT TEMPERATURE PROFILE BASED ON PREVIOUS
C  TIME STEP SOLID TEMPERATURE PROFILE.  ALSO GENERATE NEW COOLANT
C  THERMAL CONDUCTIVITIES, AVERAGE VISCOSITY, AND AVERAGE DENSITY
C
        CALL TLIQUID(TSOLD, TLOLD, KL, MULAVG, RHOLAVG, TLNEW)
C
C  CALCULATE A NEW SOLID TEMPERATURE PROFILE BASED ON NEW COOLANT
C  TEMPERATURE PROFILE, AND COOLANT THERMAL CONDUCTIVITIES
C
        CALL TSOLID(TSOLD, TLOLD, KL, TSNEW)
C
C  INITIALIZE THE SUM OF THE SQUARES DIFFERENCES, DELTAS AND DELTAL
C  TO ZERO BEFORE SUMMING TERMS
C
        DELTAS = 0.0
        DELTAL = 0.0
C
C  SUM UP THE SQUARES OF THE DIFFERENCES BETWEEN THE SOLID AND COOLANT
C  TEMPERATURES
C
        DO N=1,(LASTX+1)
          M = N + 2
          DELTAS = DELTAS + ((TSNEW(N)-TSOLD(N))**2.0)
          DELTAL = DELTAL + ((TLNEW(M)-TLOLD(M))**2.0)
        END DO
C
C  THE TOLERANCE VARIABLE, DIFF, IS ASSIGNED THE SUM OF THE SQUARES
C
        DIFF = DELTAS + DELTAL
C
C  ASSIGN THE NEW TIME STEP VALUES TO THE PREVIOUS TIME STEP VARIABLES
C
        DO N=1,(LASTX+1)
          M = N + 2
          TSOLD(N) = TSNEW(N)
          TLOLD(M) = TLNEW(M)
        END DO
```

```
C
C  INCREMENT THE ITERATION COUNTER
C
      STEP = STEP+1
C
C  END THE MAIN LOOP
C
    END DO
C
C  SEND THE NEWEST TEMPERATURE PROFILES TO THE OUTPUT SUBROUTINE TO
C  BE STORED IN A FILE
C
    CALL OUTPUT(TSNEW, TLNEW)
C
C  END THE MAIN PROGRAM
C
    STOP
    END
C
C  THIS SUBROUTINE PROVIDES THE INITIAL CONDITIONS AND CONSTANTS
C  USED IN THE REST OF THE PROGRAM
C
    SUBROUTINE INPUT(TSOLD, TLOLD, RHOLAVG, MULAVG, DIFFLIM, TLNEW)

    IMPLICIT NONE
C
C  VARIABLES USED IN INPUT
C
C    TSOLD = VECTOR OF POROUS SOLID TEMPERATURE AT PREVIOUS TIME STEP
C    TLOLD = VECTOR OF TRANSPIRATION COOLANT TEMPERATURE AT PREVIOUS
C          TIME STEP
C    EPS = POROSITY OF THE POROUS SOLID
C    R = POROUS SPHERE RADIUS
C    TB = BULK TEMPERATURE OF THE COOLANT IN THE COOLANT CHANNEL
C    DX = X DISTANCE STEP SIZE THROUGH WALL
C    C0 = PROPORTIONALITY CONSTANT USED TO DETERMINE SOLID SURFACE AREA
C    MDOTC = MASS FLOW RATE OF COOLANT IN COOLANT CHANNEL
C    DH = HYDRAULIC DIAMETER OF COOLANT CHANNEL
C    PB = COOLANT LINE PRESSURE (BULK CONDITIONS)
C    PI = 3.14159
C    THROATD = NOZZLE AERODYNAMIC THROAT DIAMETER
C    MDOTF = MASS FLOW RATE OF COMBUSTION PRODUCTS
C    W = VISCOSITY, TEMPERATURE EXPONENT
C    PH = HYDRAULIC PERIMETER OF COOLANT CHANNEL
C    GAM = RATIO OF SPECIFIC HEATS OF COMBUSTION PRODUCTS
C    T0G = STAGNATION TEMPERATURE OF COMBUSTION PRODUCTS
C    TG = STATIC TEMPERATURE OF COMBUSTION PRODUCTS AT THROAT
C    DELTAP = CHANGE IN PRESSURE ACROSS THE POROUS WALL
C    THICKNESS = POROUS NOZZLE WALL THICKNESS AT THROAT
C    PERMEABLE = POROUS WALL PERMEABILITY
```

```
C    RHOLAVG = AVERAGE COOLANT DENSITY
C    MULAVG = AVERAGE COOLANT VISCOSITY
C    PLAVG = AVERAGE PRESSURE WITHIN POROUS WALL
C    PTHROAT = STATIC THROAT PRESSURE
C    RHOB = COOLANT DENSITY AT BULK CONDITIONS
C    DP = PRESSURE STEP SIZE THROUGH WALL
C    RHOS = SOLID DENSITY
C    CPS = SOLID SPECIFIC HEAT
C    KW = SOLID THERMAL CONDUCTIVITY
C    MUB = COOLANT VISCOSITY AT BULK CONDITIONS
C    KB = COOLANT THERMAL CONDUCTIVITY AT BULK CONDITIONS
C    CPB = COOLANT SPECIFIC HEAT, CONSTANT PRESSURE, AT BULK CONDITIONS
C    DIFFLIM = SPECIFIED TOLERANCE USED TO DETERMINE CONVERGENCE
C    PBB = COOLANT CHANNEL PRESSURE FOR REGENERATIVE COOLING CASE
C    TLAVG = AVERAGE COOLANT TEMPERATURE THROUGH POROUS WALL
C    MU0F = COMBUSTION PRODUCTS VISCOSITY AT T0G
C    CP0F = COMBUSTION PRODUCTS SPECIFIC HEAT AT T0G
C    PR0F = COMBUSTION PRODUCTS PRANDTL NUMBER AT T0G
C    TLNEW = COOLANT TEMPERATURE AT NEW TIME STEP
C    KLAVG = COOLANT THERMAL CONDUCTIVITY AT TLAVG AND PLAVG
C    CPLAVG = COOLANT SPECIFIC HEAT AT TLAVG AND PLAVG
C    TLSTART = INITIAL COOLANT TEMPERATURE AT FIRST GRID POINT
C    TLEND = INITIAL COOLANT TEMPERATURE AT LAST GRID POINT
C    DTEMP = INCREMENTAL CHANGE IN TEMPERATURE FOR INITIAL PROFILE
C    HCL = PACKED BED OF SPHERES HEAT TRANSFER COEFFICIENT
C    MDOTL = MASS FLOW RATE OF COOLANT THROUGH POROUS WALL
C    N = INDEX USED FOR SOLID TEMPERATURE ARRAY
C    M = INDEX USED FOR COOLANT TEMPERATURE ARRAY
C    LASTX = GRID SIZE
C    FILE1 = FILENAME USED TO STORE OUTPUT
C
C  DECLARE THE VARIABLES
C
     DOUBLE PRECISION TSOLD, TLOLD, EPS, R, TB, DX, C0
     DOUBLE PRECISION MDOTC, DH, PB, PI, THROATD, MDOTF, W, PH
     DOUBLE PRECISION GAM, T0G, TG, DELTAP, THICKNESS, PERMEABLE
     DOUBLE PRECISION RHOLAVG, MULAVG, PLAVG, PTHROAT, RHOB
     DOUBLE PRECISION DP, RHOS, CPS, KW, MUB, KB, CPB, DIFFLIM
     DOUBLE PRECISION PBB, TLAVG, MU0F, CP0F, PR0F, TLNEW
     DOUBLE PRECISION KLAVG, CPLAVG, TLSTART, TLEND, DTEMP
     DOUBLE PRECISION HCL, MDOTL

     INTEGER LASTX, N, M

     CHARACTER*64 FILE1
C
C  DIMENSION THE VARIABLES THAT ARE ARRAYS
C
     DIMENSION TSOLD(20000), TLOLD(20000), TLNEW(20000)
C
```

```
C  THIS COMMON BLOCK CONTAINS THE GRID DIMENSIONS USED
C
      COMMON /DIMEN/ LASTX, DX
C
C  THIS COMMON BLOCK CONTAINS THE OUTPUT FILENAME
C
      COMMON /FILEBLK/ FILE1
C
C  THIS COMMON BLOCK CONTAINS VARIABLES COMMON TO TSOLID AND TLIQUID
C
      COMMON /TSTL/ C0, EPS, R, PB, TB, KW, HCL, MDOTL
C
C  THIS COMMON BLOCK CONTAINS VARIABLES USED IN TLIQUID ONLY
C
      COMMON /TLBLK/ PLAVG, TLAVG, RHOB, DP,DELTAP,PERMEABLE,THICKNESS
C
C  THIS COMMON BLOCK CONTAINS VARIABLES USED IN TSOLID ONLY
C
      COMMON /TSBLK/ RHOS, CPS, MDOTC, DH, PI, THROATD, MDOTF
      COMMON /TSBLK/ PH, W, GAM, T0G, TG, PBB, MU0F, CP0F, PR0F
C
C  SPECIFY CONSTANT VALUES
C
      PTHROAT = 11.890000000D6
      PBB = 41.37D6
      THICKNESS = 7.112D-4
      TB = 138.89
      T0G = 3656.7
      TG = 3439.4
      W = 0.875
      GAM = 1.1481
      MDOTF = 468.3134
      THROATD = 0.26006
      PI = 3.14159
      DH = 1.45143D-03
      PH = 7.112D-03
      MDOTC = 3.344D-02
      RHOS = 19300.0
      CPS = 129.0
      MU0F = 1.10236699599D-4
      CP0F = 3740.68492
      PR0F = 0.6151
C
C  READ IN VARIABLES SPECIFIC TO THIS RUN
C
      READ (*,1) FILE1
      READ (*,*) DIFFLIM
      READ (*,*) LASTX
      READ (*,*) PB
      READ (*,*) R
```

```
      READ (*,*) C0
      READ (*,*) EPS
      READ (*,*) KW
C
C  GENERATE HYDROGEN PROPERTIES AT BULK CONDITIONS
C
      CALL H2PROP(PB, TB, MUB, KB, RHOB, CPB)
C
C  CALCULATE THE REST OF THE NECESSARY VARIABLES FROM KNOWN VALUES
C
      PLAVG = (PB+PTHROAT)/2.0
      DX = THICKNESS/LASTX
      DELTAP = (PB-PTHROAT)
      DP = DELTAP/LASTX
      PERMEABLE = ((2.0*R)**2.0)*(EPS**3.0)/(150.0*((1.0-EPS)**2.0))
      TLSTART = 138.89
      TLEND = 700.0
      DTEMP = (TLEND-TLSTART)/LASTX
C
C  SPECIFY THE BEGINNING LIQUID AND SOLID TEMPERATURE PROFILES
C
      DO N=1,(LASTX+1)
        M = N + 2
        TLOLD(M) = TLSTART + DTEMP*(N-1)
        TSOLD(N) = TLOLD(M)+15
        TLNEW(M) = TLOLD(M)
      END DO
C
C  SPECIFY NEW AND OLD COOLANT TEMPERATURES JUST PRIOR TO THE
C  POROUS WALL SURFACE
C
      TLOLD(1) = TB
      TLOLD(2) = TB
      TLNEW(1) = TB
      TLNEW(2) = TB
C
C  CALCULATE THE AVERAGE COOLANT TEMPERATURE WITHIN THE POROUS WALL
C
      TLAVG = (TLOLD(3)+TLOLD(LASTX+3))/2.0
C
C  GENERATE HYDROGEN PROPERTIES AT THE AVERAGE PRESSURE AND TEMPERATURE
C
      CALL H2PROP(PLAVG, TLAVG, MULAVG, KLAVG, RHOLAVG, CPLAVG)
C
C  FORMAT STATEMENT FOR THE READ
C
 1    FORMAT(2(A))
      RETURN
C
C  END INPUT SUBROUTINE
```

```
C
      END
C
C  THIS SUBROUTINE GENERATES HYDROGEN THERMODYNAMIC PROPERTIES AT A
C  GIVEN PRESSURE AND TEMPERATURE
C
      SUBROUTINE H2PROP(P, TL, MU, K, RHO, CP)

      IMPLICIT NONE
C
C  VARIABLES USED IN H2PROP
C
C     P = HYDROGEN PRESSURE
C     TL = LOCAL HYDROGEN TEMPERATURE
C     MU = HYDROGEN VISCOSITY
C     K = HYDROGEN THERMAL CONDUCTIVITY
C     RHO = HYDROGEN DENSITY
C     CP = HYDROGEN SPECIFIC HEAT AT CONSTANT PRESSURE
C
C  DECLARE VARIABLES
C
      DOUBLE PRECISION P, TL, MU, K, RHO, CP
C
C  CURVE FITS TO CALCULATE PROPERTIES
C
        MU = (1.28717D-15)*(TL**3.0)+
     + (-8.36499D-12)*(TL**2.0)+(2.61452D-8*TL)+2.38468D-6
        K = (-6.67524D-14)*(TL**4.0)+(2.77669D-10)*(TL**3.0)+
     + (-3.22714D-7)*(TL**2.0)+(0.00056901*TL)+0.0729104
        RHO = P/(4157.5*TL)
        CP = (-1.39859D-11)*(TL**4.0)+(1.48717D-7)*(TL**3.0)-
     + (0.000849414)*(TL**2.0)+(3.74545*TL)+12116.7
C
C  THESE VALUES REPRESENT PROPERTIES AT 600K AND 11.89D6 PA
C
C       MU = 1.5338D-5
C       K = .349464738
C       RHO = 4.76648627
C       CP = 14088.49147502
C
C  THESE VALUES REPRESENT PROPERTIES AT 138.89K AND 12.06D6 PA
C
C       MU = 5.858D-6
C       K = .146434006
C       RHO = 20.885461299
C       CP = 12620.913431226
      RETURN
C
C  END H2PROP SUBROUTINE
C
```

```
      END
C
C  THIS SUBROUTINE CALCULATES THE SOLID TEMPERATURE PROFILE GIVEN
C  THE PREVIOUS TIME STEP SOLID AND COOLANT TEMPERATURE PROFILES, AND
C  THE LIQUID THERMAL CONDUCTIVITIES
C
      SUBROUTINE TSOLID(TSOLD, TLOLD, KL, TSNEW)

      IMPLICIT NONE
C
C  VARIABLES USED IN TSOLID
C
C     TSOLD = VECTOR OF POROUS SOLID TEMPERATURE AT PREVIOUS TIME STEP
C     KL = LOCAL COOLANT THERMAL CONDUCTIVITY
C     DT = TIME STEP
C     DX = X DISTANCE STEP SIZE THROUGH WALL
C     HCL = PACKED BED OF SPHERES HEAT TRANSFER COEFFICIENT
C     C0 = PROPORTIONALITY CONSTANT USED TO DETERMINE SOLID SURFACE AREA
C     R = POROUS SPHERE RADIUS
C     EPS = POROSITY OF THE POROUS SOLID
C     TLOLD = VECTOR OF TRANSPIRATION COOLANT TEMPERATURE AT PREVIOUS
C           TIME STEP
C     TB = BULK TEMPERATURE OF THE COOLANT IN THE COOLANT CHANNEL
C     MDOTC = MASS FLOW RATE OF COOLANT IN COOLANT CHANNEL
C     DH = HYDRAULIC DIAMETER OF COOLANT CHANNEL
C     PB = COOLANT LINE PRESSURE (BULK CONDITIONS)
C     PI = 3.14159
C     THROATD = NOZZLE AERODYNAMIC THROAT DIAMETER
C     MDOTF = MASS FLOW RATE OF COMBUSTION PRODUCTS
C     W = VISCOSITY, TEMPERATURE EXPONENT
C     PH = HYDRAULIC PERIMETER OF COOLANT CHANNEL
C     PBB = COOLANT CHANNEL PRESSURE FOR REGENERATIVE COOLING CASE
C     GAM = RATIO OF SPECIFIC HEATS OF COMBUSTION PRODUCTS
C     T0G = STAGNATION TEMPERATURE OF COMBUSTION PRODUCTS
C     MDOTL = MASS FLOW RATE OF COOLANT THROUGH POROUS WALL
C     TG = STATIC TEMPERATURE OF COMBUSTION PRODUCTS AT THROAT
C     TSNEW = SOLID TEMPERATURE AT NEW TIME STEP
C     RHOS = SOLID DENSITY
C     CPS = SOLID SPECIFIC HEAT
C     KW = SOLID THERMAL CONDUCTIVITY
C     KS = EFFECTIVE THERMAL CONDUCTIVITY OF THE POROUS SOLID
C     HCS = COLD GAS SIDE HEAT TRANSFER COEFFICIENT
C     TWH = HOT GAS SIDE SOLID WALL TEMPERATURE
C     TAW = ADIABATIC WALL TEMPERATURE
C     HG = HOT GAS SIDE HEAT TRANSFER COEFFICIENT
C     STAB1 = STABILITY CONSTRAINT
C     STAB2 = STABILITY CONSTRAINT
C     STAB3 = STABILITY CONSTRAINT
C     MU0F = COMBUSTION PRODUCTS VISCOSITY AT T0G
C     CP0F = COMBUSTION PRODUCTS SPECIFIC HEAT AT T0G
```

```
C    PR0F = COMBUSTION PRODUCTS PRANDTL NUMBER AT T0G
C    N = INDEX USED FOR SOLID TEMPERATURE ARRAY
C    M = INDEX USED FOR COOLANT TEMPERATURE ARRAY
C    LASTX = GRID SIZE
C
C  DECLARE VARIABLES
C
     DOUBLE PRECISION TSOLD, KL, DT, DX, HCL, C0, R, EPS, TLOLD, TB
     DOUBLE PRECISION MDOTC, DH, PB, PI, THROATD, MDOTF, W, PH, PBB
     DOUBLE PRECISION GAM, T0G, MDOTL, TG, TSNEW, RHOS, CPS, KW
     DOUBLE PRECISION KS, HCS, TWH, TAW, HG, STAB1, STAB2, STAB3
     DOUBLE PRECISION MU0F, CP0F, PR0F

     INTEGER N, M, LASTX
C
C  DIMENSION VARIABLES THAT ARE ARRAYS
C
     DIMENSION TSOLD(20000), KL(20000), TLOLD(20000)
     DIMENSION TSNEW(20000)
C
C  THIS COMMON BLOCK CONTAINS THE GRID DIMENSIONS USED
C
     COMMON /DIMEN/ LASTX, DX
C
C  THIS COMMON BLOCK CONTAINS OUTPUT VARIABLES FROM TSOLID
C
     COMMON /SOLBLK/ HCS, HG, TAW
C
C  THIS COMMON BLOCK CONTAINS VARIABLES COMMON TO TSOLID AND TLIQUID
C
     COMMON /TSTL/ C0, EPS, R, PB, TB, KW, HCL, MDOTL
C
C  THIS COMMON BLOCK CONTAINS VARIABLES COMMON TO TSOLID ONLY
C
     COMMON /TSBLK/ RHOS, CPS, MDOTC, DH, PI, THROATD, MDOTF
     COMMON /TSBLK/ PH, W, GAM, T0G, TG, PBB, MU0F, CP0F, PR0F
C
C  BEGIN THE MAIN LOOP TO MARCH THROUGH THE POROUS WALL
C
     DO N=1,(LASTX+1)
C
C  SYNCHRONIZE THE LIQUID AND SOLID INDICES
C
       M = N + 2
C
C  CALCULATE THE EFFECTIVE THERMAL CONDUCTIVITY OF THE SOLID
C
       KS = KL(N)*((2.0*KL(N)+KW)-2.0*(1.0-EPS)*(KL(N)-KW))/
    + (2.0*KL(N)+KW+(1.0-EPS)*(KL(N)-KW))
C
```

```
C  INITIALIZE THE STABILITY CONSTRAINT CONSTANTS
C
      STAB1 = 1.0
      STAB2 = 1.0
      STAB3 = 1.0
C
C  IF CALCULATING THE COLD GAS SIDE BOUNDARY TEMPERATURE USE THIS
C  IF-THEN LOOP
C
      IF (N.EQ.1) THEN
C
C  GENERATE THE COLD GAS SIDE HEAT TRANSFER COEFFICIENT
C
         CALL HCOOLSIDE(PBB, TB, TSOLD(N), MDOTC, DH, PH, HCS)
C
C  GENERATE THE STABLE TIME STEP FOR THIS LOCATION
C
         DT = 0.9/((2.0*KS)/((DX**2.0)*RHOS*CPS)+
     + (HCL*C0)/(RHOS*R*CPS)+(2.0*HCS)/(RHOS*DX*CPS))
C
C  CALCULATE THE NEW TEMPERATURE AT THE COLD GAS SIDE BOUNDARY
C
         TSNEW(N) = ((2.0*KS*DT)/((DX**2.0)*RHOS*CPS))*(TSOLD(N+1)
     + -TSOLD(N))-((HCL*C0*DT)/(RHOS*R*CPS))*(TSOLD(N)-
     + TLOLD(M))-((2.0*HCS*DT)/(RHOS*DX*CPS))*(TSOLD(N)-TB)+TSOLD(N)
C
C  CALLCULATE STABILITY CONSTRAINT
C
         STAB1 = 1.0/((2.0*KS)/((DX**2.0)*RHOS*CPS)+
     + (HCL*C0)/(RHOS*R*CPS)+(2.0*HCS)/(RHOS*DX*CPS))
      END IF
C
C  IF CALCULATING AN INTERIOR NODE POINT USE THIS IF-THEN LOOP
C
      IF ((N.NE.1).AND.(N.NE.(LASTX+1))) THEN
C
C  CALCULATE THE TIME STEP FOR THIS LOCATION
C
         DT = 0.9/((2.0*KS)/((DX**2.0)*RHOS*CPS)+
     + (HCL*C0)/(RHOS*R*CPS))
C
C  CALCULATE THE NEW TEMPERATURE AT THIS LOCATION
C
         TSNEW(N) = ((KS*DT)/((DX**2.0)*RHOS*CPS))*(TSOLD(N+1)+
     + TSOLD(N-1)-2.0*TSOLD(N))-((HCL*C0*DT)/(RHOS*R*CPS))*
     + (TSOLD(N)-TLOLD(M))+TSOLD(N)
C
C  CALCULATE STABILITY CONSTRAINT
C
         STAB2 = 1.0/((2.0*KS)/((DX**2.0)*RHOS*CPS)+
```

```
     + (HCL*C0)/(RHOS*R*CPS))
        END IF
C
C  IF CALCULATING THE HOT GAS SIDE BOUNDARY TEMPERATURE THEN USE
C  THIS IF-THEN LOOP
C
        IF (N.EQ.(LASTX+1)) THEN
C
C  ASSIGN THE PREVIOUS TIME STEP TEMPERATURE TO THE HOT GAS SIDE
C  WALL TEMPERATURE
C
          TWH = TSOLD(N)
C
C  GENERATE THE HOT GAS SIDE HEAT TRANSFER COEFFICIENT
C
          CALL HOTGAS(TWH, THROATD, MDOTF, W, GAM, T0G, TG,
     + MDOTL, PI, EPS, TAW, MU0F, CP0F, PR0F, HG)
C
C  CALCULATE A TIME STEP FOR THIS LOCATION
C
          DT = 0.9/((2.0*KS)/((DX**2.0)*RHOS*CPS)+
     + (HCL*C0)/(RHOS*R*CPS)+(2.0*HG)/(RHOS*DX*CPS))
C
C  CALCULATE THE NEW TEMPERATURE AT THIS LOCATION
C
          TSNEW(N) = ((2.0*HG*DT)/(RHOS*DX*CPS))*(TAW-TSOLD(N))-
     + ((HCL*C0*DT)/(RHOS*R*CPS))*(TSOLD(N)-TLOLD(M))-
     + ((2.0*KS*DT)/((DX**2.0)*RHOS*CPS))*(TSOLD(N)-TSOLD(N-1))+TSOLD(N)
C
C  CALCULATE STABILITY CONSTRAINT
C
          STAB3 = 1.0/((2.0*KS)/((DX**2.0)*RHOS*CPS)+
     + (HCL*C0)/(RHOS*R*CPS)+(2.0*HG)/(RHOS*DX*CPS))
        END IF
C
C  CHECK TIME STEPS AGAINST STABILITY CONSTRAINTS TO PREVENT INSTABILITY
C  IF IT FAILS, THE PROGRAM WRITES THE FOLLOWING OUTPUT AND STOPS THE
PROGRAM
C
      IF ((DT.GT.STAB1).OR.(DT.GT.STAB2).OR.(DT.GT.STAB3)) THEN
        WRITE (*,*) 'STABILITY CONSTRAINT VIOLATION'
        WRITE (*,*) 'STAB1 = ', STAB1
        WRITE (*,*) 'STAB2 = ', STAB2
        WRITE (*,*) 'STAB3 = ', STAB3
        WRITE (*,*) 'DT USED = ',DT
        CLOSE(14)
        STOP
      END IF
C
C  END THE MAIN LOOP
```

```
C
      END DO
      RETURN
C
C  END TSOLID SUBROUTINE
C
      END
C
C  THIS SUBROUTINE CALCULATES THE COLD GAS SIDE HEAT TRANSFER
C  COEFFICIENT GIVEN COOLANT BULK PRESSURE AND TEMPERATURE,
C  POROUS SOLID TEMPERATURE, MASS FLOW RATE THROUGH THE COOLANT
C  CHANNEL, AND HYDRAULIC DIAMETER AND PERIMETER
C
      SUBROUTINE HCOOLSIDE(PB, TB, TS, MDOT, DH, PH, HCS)

      IMPLICIT NONE
C
C  VARIABLES USED IN HCOOLSIDE
C
C     PB = COOLANT LINE PRESSURE (BULK CONDITIONS)
C     TB = COOLANT BULK TEMPERATURE IN COOLANT CHANNEL
C     TS = SURFACE TEMPERATURE OF POROUS SOLID ON COLD GAS SIDE
C     MDOT = MASS FLOW RATE OF COOLANT IN COOLANT CHANNEL
C     DH = HYDRAULIC DIAMETER OF COOLANT CHANNEL
C     PH = HYDRAULIC PERIMETER OF COOLANT CHANNEL
C     HCS = COLD GAS SIDE HEAT TRANSFER COEFFICIENT
C     MUB = COOLANT VISCOSITY AT BULK CONDITIONS
C     KB = COOLANT THERMAL CONDUCTIVITY AT BULK CONDITIONS
C     RHOB = COOLANT DENSITY AT BULK CONDITIONS
C     CPB = COOLANT SPECIFIC HEAT AT BULK CONDITIONS
C     MULS = COOLANT VISCOSITY AT SOLID SURFACE TEMPERATURE
C     KLS = COOLANT THERMAL CONDUCTIVITY AT SOLID SURFACE TEMPERATURE
C     RHOLS = COOLANT DENSITY AT SOLID SURFACE TEMPERATURE
C     CPLS = COOLANT SPECIFIC HEAT AT SOLID SURFACE TEMPERATURE
C     PRB = PRANDTL NUMBER AT BULK CONDITIONS
C     REDB = REYNOLD'S NUMBER AT BULK CONDITIONS
C
C  DECLARE VARIABLES
C
      DOUBLE PRECISION PB, TB, TS, MDOT, DH, PH, HCS
      DOUBLE PRECISION MUB, KB, RHOB, CPB, MULS, KLS, RHOLS, CPLS
      DOUBLE PRECISION PRB, REDB
C
C  GENERATE HYDROGEN PROPERTIES AT BULK CONDITIONS
C
      CALL H2PROP(PB, TB, MUB, KB, RHOB, CPB)
C
C  CALCULATE PRANDTL NUMBER AND REYNOLD'S NUMBER
C
      PRB = (MUB*CPB)/KB
```

```
      REDB = (4.0*MDOT)/(MUB*PH)
C
C  GENERATE HYDROGEN PROPERTIES AT SOLID SURFACE TEMPERATURE
C
      CALL H2PROP(PB, TS, MULS, KLS, RHOLS, CPLS)
C
C  CALCULATE THE COLD GAS SIDE HEAT TRANSFER COEFFICIENT
C
      HCS = ((KB*0.027)/DH)*(REDB**0.8)*(PRB**(1.0/3.0))*
     + ((MUB/MULS)**.14)
      RETURN
C
C  END HCOOLSIDE SUBROUTINE
C
      END
C
C  THIS SUBROUTINE CALCULATES THE HOT GAS SIDE HEAT TRANSFER
C  COEFFICIENT INCLUDING THE EFFECT OF BLOWING RATIO
C
      SUBROUTINE HOTGAS(TWH, THROATD, MDOT, W, GAM, T0G, TG,
     + MDOTL, PI, EPS, TAW, MU0F, CP0F, PR0F, HG)

      IMPLICIT NONE
C
C  VARIABLES USED IN HOTGAS
C
C    TWH = HOT GAS SIDE SOLID SURFACE TEMPERATURE
C    THROATD = NOZZLE AERODYNAMIC THROAT DIAMETER
C    MDOT = COMBUSTION GAS MASS FLOW RATE
C    W = VISCOSITY, TEMPERATURE EXPONENT
C    GAM = RATIO OF SPECIFIC HEATS FOR COMBUSTION GASES
C    T0G = COMBUSTION GAS STAGNATION TEMPERATURE
C    TG = COMBUSTION GAS STATIC TEMPERATURE AT THROAT
C    MDOTL = COOLANT MASS FLOW RATE THROUGH POROUS WALL
C    PI = 3.14159
C    EPS = POROSITY
C    TAW = ADIABATIC WALL TEMPERATURE
C    HG = HOT GAS SIDE HEAT TRANSFER COEFFICIENT
C    AT = NOZZLE AERODYNAMIC THROAT AREA
C    MU0F = COMBUSTION GAS VISCOSITY AT STAGNATION TEMPERATURE
C    CP0F = COMBUSTION GAS SPECIFIC HEAT AT STAGNATION TEMPERATURE
C    BR = BLOWING RATIO
C    SIGMA = BARTZ' EQUATION CONSTANT
C    HG0 = HOT GAS SIDE HEAT TRANSFER COEFFICIENT WITHOUT BLOWING
C    PR0F = COMBUSTION GAS PRANDTL NUMBER AT STAGNATION TEMPERATURE
C    RHOFUF = MASS FLUX OF COMBUSTION GASES
C
C  DECLARE VARIABLES
C
      DOUBLE PRECISION TWH, THROATD, MDOT, W, GAM, T0G, TG
```

```
      DOUBLE PRECISION MDOTL, PI, EPS, TAW, HG, AT, MU0F, CP0F
      DOUBLE PRECISION BR, SIGMA, HG0, PR0F, RHOFUF
C
C  THIS COMMON BLOCK CONTAINS OUTPUT VARIABLES FROM HOTGAS
C
      COMMON /HGBLK/ BR
C
C  CALCULATE THE AERODYNAMIC THROAT AREA
C
      AT = (PI*(THROATD**2.0))/4.0
C
C  CALCULATE THE ADIABATIC WALL TEMPERATURE
C
      CALL FINDTAW(TG, T0G, TWH, TAW)
C
C  CALCULATE THE MASS FLUX OF THE COMBUSTION GASES
C
      RHOFUF = MDOT/AT
C
C  CALCULATE THE BLOWING RATIO
C
      BR = MDOTL/(RHOFUF*EPS)
C
C  THIS LIMITER PREVENTS THE BLOWING RATIO TO EXCEED 0.01
C
      IF (BR.GE.1D-02) THEN
        WRITE (*,*) 'MDOTL ',MDOTL
        WRITE (*,*) 'BR    ',BR
        WRITE (*,*) 'THE BLOWING RATIO HAS EXCEEDED 1 PERCENT'
        STOP
      END IF
C
C  CALCULATE SIGMA
C
      SIGMA = 1.0/((((0.5*(TWH/T0G)*((GAM+1.0)/2.0)+0.5)**(0.8-0.2*W))*
     + (((GAM+1.0)/2.0)**(0.2*W)))
C
C  CALCULATE THE HEAT TRANSFER COEFFICIENT WITHOUT BLOWING EFFECTS
C
      HG0 = ((0.026/(THROATD**0.2))*(((MU0F**0.2)*CP0F)/(PR0F**0.6))*
     + ((RHOFUF)**0.8)*((2.0)**0.1))*SIGMA
C
C  INCLUDE BLOWING EFFECTS
C
      HG = HG0*(1.0-38.0*BR)
      RETURN
C
C  END HOTGAS SUBROUTINE
C
      END
```

```
C
C  THIS SUBROUTINE CALCULATES THE ADIABATIC WALL TEMPERATURE
C
      SUBROUTINE FINDTAW(TG, T0G, TWH, TAW)

      IMPLICIT NONE
C
C  VARIABLES USED IN FINDTAW
C
C     TG = STATIC COMBUSTION GAS TEMPERATURE AT THROAT
C     T0G = COMBUSTION GAS STAGNATION TEMPERATURE
C     TWH = HOT GAS SIDE SOLID SURFACE TEMPERATURE
C     TAW = ADIABATIC WALL TEMPERATURE
C     DELTA = CONVERGENCE CRITERIA
C     TFNEW = NEW FILM TEMPERATURE
C     TFOLD = OLD FILM TEMPERATURE
C     MUF = COMBUSTION GAS VISCOSITY AT FILM TEMPERATURE
C     CPF = COMBUSTION GAS SPECIFIC HEAT AT FILM TEMPERATURE
C     KF = COMBUSTION GAS THERMAL CONDUCTIVITY AT FILM TEMPERATURE
C     PRF = COMBUSTION GAS PRANDTL NUMBER AT FILM TEMPERATURE
C
C  DECLARE VARIABLES
C
      DOUBLE PRECISION TG, T0G, TWH, TAW, DELTA, TFNEW, TFOLD, MUF
      DOUBLE PRECISION CPF, KF, PRF
C
C  INITIALIZE VARIABLES
C
      DELTA = 9999.0
      TFOLD = (TWH+T0G)/2.0
C
C  BEGIN MAIN LOOP AND ITERATE UNTIL CONVERGED ON CORRECT FILM
C  TEMPERATURE
C
      DO WHILE (DELTA.GE.1D-04)
C
C  GENERATE COMBUSTION GAS PROPERTIES AT OLD FILM TEMPERATURE
C
        CALL HOTGASPROP(TFOLD, MUF, CPF, KF)
C
C  CALCULATE NEW PRANDTL NUMBER, ADIABATIC WALL TEMPERATURE AND
C  FILM TEMPERATURE
C
        PRF = (MUF*CPF)/KF
        TAW = (PRF**(1.0/3.0))*(T0G-TG)+TG
        TFNEW = TWH+0.23*(TG-TWH)+0.19*(TAW-TWH)
C
C  COMPARE OLD AND NEW FILM TEMPERATURES TO CHECK FOR CONVERGENCE
C
        DELTA = (TFNEW-TFOLD)**2.0
```

```
      TFOLD = TFNEW
C
C  END MAIN LOOP
C
      END DO
      RETURN
C
C  END FINDTAW SUBROUTINE
C
      END
C
C  THIS SUBROUTINE GENERATES THE COMBUSTION GAS PROPERTIES AT
C  DIFFERENT TEMPERATURES
C
      SUBROUTINE HOTGASPROP(T, MUF, CPF, KF)

      IMPLICIT NONE
C
C  VARIABLES USED IN HOTGASPROP
C
C     T = LOCAL STATIC TEMPERATURE AT THROAT
C     MUF = COMBUSTION GAS VISCOSITY
C     CPF = COMBUSTION GAS SPECIFIC HEAT
C     KF = COMBUSTION GAS THERMAL CONDUCTIVITY
C     PRF = COMBUSTION GAS PRANDTL NUMBER
C
C  DECLARE VARIABLES
C
      DOUBLE PRECISION T, MUF, CPF, KF, PRF
C
C  GENERATE THERMODYNAMIC PROPERTIES
C
      MUF = (-3.19123D-12)*(T**2.0)+(4.21474D-08)*T-(1.91043D-06)
      CPF = (-1.76051D-13)*(T**5.0)+(2.389596D-09)*(T**4.0)
     + -(1.12842D-05)*(T**3.0)+(0.0240347)*(T**2.0)-(22.7384*T)+
     + 10438
      PRF = (-3.63422D-27)*(T**8.0)+(6.93638D-23)*(T**7.0)-
     + (5.70795D-19)*(T**6.0)+(2.63999D-15)*(T**5.0)-
     + (7.47121D-12)*(T**4.0)+(1.31513D-8)*(T**3.0)-
     + (1.39728D-5)*(T**2.0)+(0.00818492)*T-1.4202
      KF = MUF*CPF/PRF
      RETURN
C
C  END HOTGASPROP SUBROUTINE
C
      END
C
C  THIS SUBROUTINE SENDS THE TEMPERATURE PROFILES TO THE SPECIFIED
C  FILENAME, AND THE SCREEN
C
```

```
      SUBROUTINE OUTPUT(TSNEW, TLNEW)

      IMPLICIT NONE
C
C  VARIABLES USED IN OUTPUT
C
C     DX = INCREMENTAL DISTANCE STEP
C     TSNEW = SOLID TEMPERATURE PROFILE AT NEW TIME STEP
C     TLNEW = COOLANT TEMPERATURE PROFILE AT NEW TIME STEP
C     PB = COOLANT LINE PRESSURE
C     R = POROUS SPHERE RADIUS
C     C0 = PROPORTIONALITY CONSTANT FOR POROUS SOLID SURFACE AREA
C     EPS = POROSITY
C     KW = SOLID THERMAL CONDUCTIVITY
C     MDOTL = COOLANT MASS FLOW RATE THROUGH POROUS SOLID
C     BR = BLOWING RATIO
C     HCS = COLD GAS SIDE HEAT TRANSFER COEFFICIENT
C     HG = HOT GAS SIDE HEAT TRANSFER COEFFICIENT
C     HCL = PACKED BED OF SPHERES HEAT TRANSFER COEFFICIENT
C     TAW = ADIABATIC WALL TEMPERATURE
C     TB = COOLANT BULK TEMPERATURE
C     N = INDEX USED FOR SOLID TEMPERATURE ARRAY
C     M = INDEX USED FOR COOLANT TEMPERATURE ARRAY
C     LASTX = GRID SIZE
C     FILE1 = OUTPUT FILENAME
C
C  DECLARE VARIABLES
C
      DOUBLE PRECISION DX, TSNEW, TLNEW, PB, R, C0, EPS, KW
      DOUBLE PRECISION MDOTL, BR, HCS, HG, HCL, TAW, TB

      INTEGER N, M, LASTX

      CHARACTER*64 FILE1
C
C  DIMENSION VARIABLES THAT ARE ARRAYS
C
      DIMENSION TSNEW(20000), TLNEW(20000)
C
C  THIS COMMON BLOCK CONTAINS THE GRID DIMENSIONS
C
      COMMON /DIMEN/ LASTX, DX
C
C  THIS COMMON BLOCK CONTAINS VARIABLES COMMON TO TSOLID AND TLIQUID
C
      COMMON /TSTL/ C0, EPS, R, PB, TB, KW, HCL, MDOTL
C
C  THIS COMMON BLOCK CONTAINS THE OUTPUT FILENAME
C
      COMMON /FILEBLK/ FILE1
```

```
C
C  THIS COMMON BLOCK CONTAINS OUTPUT DATA FROM HOTGAS
C
     COMMON /HGBLK/ BR
C
C  THIS COMMON BLOCK CONTAINS OUTPUT DATA FROM TSOLID
C
     COMMON /SOLBLK/ HCS, HG, TAW
C
C  OPEN THE OUTPUT FILE
C
     OPEN (UNIT=14, FILE=FILE1)
C
C  WRITE THE DATA TO THE OUTPUT FILE
C
     DO N=1,(LASTX+1)
       M = N+2
       WRITE (14,10) 1000.0*(N-1)*DX, TSNEW(N), TLNEW(M)
     END DO

     CLOSE(14)
C
C  WRITE THE INPUT DATA AND OTHER VARIABLES TO THE SCREEN
C
     WRITE (*,*) 'INPUT VARIABLES'
     WRITE (*,*)
     WRITE (*,*) 'PB   = ',PB
     WRITE (*,*) 'R    = ',R
     WRITE (*,*) 'C0   = ',C0
     WRITE (*,*) 'EPS  = ',EPS
     WRITE (*,*) 'KW   = ',KW
     WRITE (*,*)
     WRITE (*,*) 'DATA IS STORED IN FILE = ',FILE1
     WRITE (*,*)
     WRITE (*,*) 'MDOTL = ',MDOTL
     WRITE (*,*) 'BR   = ',BR
     WRITE (*,*) 'HCS  = ',HCS
     WRITE (*,*) 'HCL  = ',HCL
     WRITE (*,*) 'HG   = ',HG
     WRITE (*,*) 'TAW  = ',TAW
C
C  FORMATTED OUTPUT STATEMENT
C
 10   FORMAT (1X,F10.8,1X,F15.9,1X,F15.9)
     RETURN
C
C  END OUTPUT SUBROUTINE
C
     END
C
```

```
C  THIS SUBROUTINE CALCULATES THE COOLANT TEMPERATURE PROFILE
C
      SUBROUTINE TLIQUID(TSOLD, TLOLD, KL, MULAVG, RHOLAVG, TLNEW)

      IMPLICIT NONE
C
C  VARIABLES USED IN TLIQUID
C
C     TLOLD = COOLANT TEMPERATURE PROFILE AT PREVIOUS TIME STEP
C     MDOTL = COOLANT MASS FLOW RATE THROUGH POROUS SOLID
C     EPS = POROSITY
C     R = POROUS SPHERE RADIUS
C     TB = COOLANT BULK TEMPERATURE
C     DX = INCREMENTAL DISTANCE STEP SIZE
C     C0 = PROPORTIONALITY CONSTANT FOR SOLID SURFACE AREA
C     TSOLD = SOLID TEMPERATURE PROFILE AT PREVIOUS TIME STEP
C     KL = COOLANT THERMAL CONDUCTIVITIES
C     RHOL = COOLANT DENSITIES
C     MULAVG = AVERAGE COOLANT VISCOSITY
C     RHOLAVG = AVERAGE COOLANT DENSITY
C     TLNEW = COOLANT TEMPERATURE PROFILE AT NEW TIME STEP
C     KW = SOLID THERMAL CONDUCTIVITY
C     DELTAP = PRESSURE DIFFERENCE ACROSS POROUS WALL
C     PERMEABLE = PERMEABILITY
C     PL = LOCAL COOLANT PRESSURE
C     KLL = LOCAL COOLANT THERMAL CONDUCTIVITY
C     CPL = COOLANT SPECIFIC HEATS
C     UL = COOLANT VELOCITIES
C     HCL = PACKED BED OF SPHERES HEAT TRANSFER COEFFICIENT
C     PB = COOLANT CHANNEL PRESSURE
C     DP = INCREMENTAL PRESSURE DIFFERENCE
C     C1, C2, C3 = PLACE HOLDER CONSTANTS
C     PLAVG = AVERAGE COOLANT PRESSURE WITHIN POROUS WALL
C     TLAVG = AVERAGE COOLANT TEMPERATURE WITHIN POROUS WALL
C     RHOB = COOLANT DENSITY AT BULK CONDITIONS
C     THICKNESS = POROUS WALL THICKNESS
C     MULL = LOCAL COOLANT VISCOSITY
C     CPLL = LOCAL COOLANT SPECIFIC HEAT
C     ULL = LOCAL COOLANT VELOCITY
C     CPLAVG = AVERAGE COOLANT SPECIFIC HEAT
C     KLAVG = AVERAGE COOLANT THERMAL CONDUCTIVITY
C     N = INDEX USED FOR SOLID TEMPERATURE ARRAY
C     M = INDEX USED FOR COOLANT TEMPERATURE ARRAY
C     LASTX = GRID SIZE
C
C  DECLARE VARIABLES
C
      DOUBLE PRECISION TLOLD, MDOTL, EPS, R, TB, DX, C0, TSOLD, KL, RHOL
      DOUBLE PRECISION MULAVG, RHOLAVG, TLNEW, KW, DELTAP, PERMEABLE
      DOUBLE PRECISION PL, KLL, RHOLL, CPL, UL, HCL, PB, DP
```

```
      DOUBLE PRECISION C1, C2, C3, PLAVG, TLAVG, RHOB, THICKNESS
      DOUBLE PRECISION MULL, CPLL, ULL, CPLAVG, KLAVG

      INTEGER N, M, LASTX
C
C  DIMENSION VARIABLES THAT ARE ARRAYS
C
      DIMENSION TLOLD(20000), TSOLD(20000), KL(20000)
      DIMENSION RHOL(20000), CPL(20000), UL(20000)
      DIMENSION TLNEW(20000)
C
C  THIS COMMON BLOCK CONTAINS THE GRID DIMENSIONS
C
      COMMON /DIMEN/ LASTX, DX
C
C  THIS COMMON BLOCK CONTAINS VARIABLES COMMON TO TSOLID AND TLIQUID
C
      COMMON /TSTL/ C0, EPS, R, PB, TB, KW, HCL, MDOTL
C
C  THIS COMMON BLOCK CONTAINS VARIABLES COMMON TO TLIQUID ONLY
C
      COMMON /TLBLK/ PLAVG, TLAVG, RHOB,DP,DELTAP,PERMEABLE,THICKNESS
C
C  CALCULATE THE COOLANT MASS FLOW RATE THROUGH THE POROUS WALL
C
      MDOTL = (DELTAP*PERMEABLE*RHOLAVG)/(THICKNESS*MULAVG)
C
C  CALCULATE THE PACKED BED OF SPHERES HEAT TRANSFER COEFFICIENT
C
      CALL HCOOL(PLAVG, TLAVG, MDOTL, RHOB, EPS, R, HCL)
C
C  BEGIN MAIN LOOP TO STEP THROUGH THE POROUS WALL
C
      DO N=1,(LASTX+1)
        M = N + 2
C
C  CALCULATE THE LOCAL COOLANT PRESSURE
C
        PL = PB-(DP*(N-1))
C
C  GENERATE HYDROGEN PROPERTIES AT THE LOCAL TEMPERATURE
C
        CALL H2PROP(PL, TLOLD(M), MULL, KLL, RHOLL, CPLL)
        KL(N) = KLL
        RHOL(N) = RHOLL
        CPL(N) = CPLL
C
C  CALCULATE THE LOCAL COOLANT VELOCITY
C
        ULL = MDOTL/(EPS*RHOLL)
```

```
      UL(N) = ULL
C
C  SET THE FIRST TWO TEMPERATURES BEFORE THE POROUS WALL EQUAL
C  TO THE BULK TEMPERATURE
C
      TLNEW(1) = TB
      TLNEW(2) = TB
C
C  DEFINE THE PLACEHOLDER CONSTANTS C1 AND C2
C
      C1 = KLL/(DX**2.0)
      C2 = (RHOLL*ULL*CPLL)/DX
C
C  DEFINE THE PLACEHOLDER CONSTANT C3 BASED UPON FIRST OR LAST GRID
C  POINTS
C
      IF ((N.NE.1).AND.(N.NE.(LASTX+1))) THEN
        C3 = (HCL*C0)/(EPS*R)
      ELSE
        C3 = (HCL*C0)/(2.0*EPS*R)
      END IF
C
C  CALCULATE THE NEW COOLANT TEMPERATURE AT THIS LOCATION
C
      TLNEW(M) = (1.0/(C2+C3-C1))*(C1*(TLNEW(M-2)-
     + 2.0*TLNEW(M-1))+C2*TLNEW(M-1) + C3*TSOLD(N))
C
C  END THE MAIN LOOP
C
    END DO
C
C  CALCULATE THE AVERAGE TEMPERATURE
C
    TLAVG = (TLNEW(3) + TLNEW(LASTX+3))/2.0
C
C  GENERATE HYDROGEN PROPERTIES AT THE AVERAGE PRESSURE AND TEMPERATURE
C
    CALL H2PROP(PLAVG, TLAVG, MULAVG, KLAVG, RHOLAVG, CPLAVG)
    RETURN
C
C  END TLIQUID SUBROUTINE
C
    END
C
C  THIS SUBROUTINE CALCULATES THE PACKED BED OF SPHERES HEAT TRANSFER
C  COEFFICIENT
C
    SUBROUTINE HCOOL(PLAVG, TLAVG, MDOTL, RHOB, EPS, R, HCL)

    IMPLICIT NONE
```

```
C
C  VARIABLES USED IN HCOOL
C
C    PLAVG = AVERAGE COOLANT PRESSURE THROUGH POROUS WALL
C    TLAVG = AVERAGE COOLANT TEMPERATURE THROUGH POROUS WALL
C    MDOTL = COOLANT MASS FLOW RATE THROUGH POROUS WALL
C    PR = COOLANT PRANDTL NUMBER
C    MU = COOLANT VISCOSITY
C    K = COOLANT THERMAL CONDUCTIVITY
C    RHO = COOLANT DENSITY
C    CP = COOLANT SPECIFIC HEAT
C    EPS = POROSITY
C    R = POROUS SPHERE RADIUS
C    HCL = PACKED BED OF SPHERES HEAT TRANSFER COEFFICIENT
C    RHOB = COOLANT DENSITY AT BULK CONDITIONS
C    REDP = COOLANT REYNOLD'S NUMBER
C
C  DECLARE VARIABLES
C
     DOUBLE PRECISION PLAVG, TLAVG, MDOTL, PR, MU, K, RHO, CP
     DOUBLE PRECISION EPS, R, HCL, RHOB, REDP
C
C  GENERATE HYDROGEN PROPERTIES AT AVERAGE PRESSURE AND TEMPERATURE
C
     CALL H2PROP(PLAVG, TLAVG, MU, K, RHO, CP)
C
C  CALCULATE PRANDTL NUMBER AND REYNOLD'S NUMBER
C
     PR = (MU*CP)/K
     REDP = (2.0*R*MDOTL)/(MU*EPS*(1.0-EPS))
C
C  CALCULATE THE PACKED BED OF SPHERES HEAT TRANSFER COEFFICIENT
C
     HCL = (K/(2.0*R))*((1.0-EPS)/EPS)*(0.5*(REDP**0.5)+
    + (0.2*(REDP**(2.0/3.0))))*(PR**(1.0/3.0))
     RETURN
C
C  END HCOOL SUBROUTINE
C
     END
```

Bibliography

Anderson, Dale A., Richard H. Pletcher, and John C. Tannehill. Computational Fluid Mechanics and Heat Transfer. New York: Hemisphere Publishing Corporation, 1984.

Bartz, D. R. "Turbulent Boundary-Layer Heat Transfer from Rapidly Accelerating Flow of Rocket Combustion Gases and of Heated Air," in Advances in Heat Transfer. Eds. James P. Hartnett and Thomas F. Irvine, Jr. New York NY: Academic Press Inc.,1965. Vol. 2.

Bowman, W. Jerry, Kenneth A. Carpenter, Christopher P. Chaplin, Richard A. Dennery, David N. Keener, Robert M. Latin, Joseph L. Lenertz, Michael J. MacLachlan, Michael J. Meyer, Brad R. Thompson, and Kevin M. Vlcek. Nonchemical Rocket Propulsion. 2nd ed. Wright Patterson Air Force Base: Air Force Institute of Technology, 1994.

Brennan, Patrick J. and Edward J. Kroliczek. Heat Pipe Design Handbook. Contract NAS5-23406. Towson MD: B & K Engineering Inc., June 1979 (NTIS N81-70112). Vol. 1.

Chen, Fu-Jung. Effects of Blowing Ratios on Heat Transfer to the Throat Region of a Porous-Walled Nozzle. MS thesis, AFIT/GAE/ENY/95J-01. School of Engineering, Air Force Institute of Technology (AU), Wright-Patterson AFB OH, June 1995 (AAL-8763).

Chi, S. W. Heat Pipe Theory and Practice: A Sourcebook. New York: McGraw-Hill Book Company, 1976.

Cook, R. T. and G. A. Coffey. "Space Shuttle Orbiter Engine Main Combustion Chamber Cooling and Life," AIAA 73-1310, AIAA/SAE 9th Propulsion Conference, Las Vegas NV, 5-7 November 1973.

Griesen, Dan A. Engineer, Aerojet Corporation, Sacramento CA. Personal Correspondence. 18 August 1995.

Hill, Philip G. and Carl R. Peterson. Mechanics and Thermodynamics of Propulsion. 2nd ed. New York: Addison-Wesley Publishing Company, 1992.

Incropera, Frank P. and David P. DeWitt. Fundamentals of Heat and Mass Transfer. 3rd ed. New York: John Wiley & Sons, Inc., 1990.

Keener, David N. Investigations of Boundary Layer and Performance Effects of Transpiration Cooling through a Porous Plate in a Rocket Nozzle. MS thesis, AFIT/GA/ENY/94D-3. School of Engineering, Air Force Institute of Technology (AU), Wright-Patterson AFB OH, December 1994 (AAL-4894).

Kreith, Frank and Mark S. Bohn. Principles of Heat Transfer. 4th ed. New York: Harper & Row, Publishers, Inc., 1986.

Lenertz, Joseph L. Effects of Blowing Ratio on Heat Transfer to the Throat Region of a Porous-Walled Nozzle. MS thesis, AFIT/GA/ENY/94D-7. School of Engineering, Air Force Institute of Technology (AU), Wright-Patterson AFB OH, December 1994 (AAL-4880).

May, Lee and Wendel M. Burkhardt. "Transpiration Cooled Throat for Hydrocarbon Rocket Engines." Contract NAS 8-36952. Sacramento CA: Aerojet Propulsion Division, December 1991 (AD-A244 255).

Mueggenburg, H. H., J. W. Hidahl, E. L. Kessler, and D. C. Rousar. "Platelet Actively Cooled Thermal Management Devices," AIAA 92-3127, AIAA/SAE/ASME/ASEE 28th Joint Propulsion Conference and Exhibit, Nashville TN, 6-8 July 1992.

Murphy, M, R. E. Anderson, D. C. Rousar, J. A. Van Kleeck. "Effects of Oxygen/Hydrogen Combustion Chamber Environment on Copper Alloys." Technical Paper for the Advanced Earth-to-Orbit Propulsion Technology Conference, Marshall Space Flight Center, Huntsville AL. May 1986.

Parks, Kim. Engineer, National Aeronautics and Space Administration, Marshall Space Flight Center, Huntsville AL. Personal Correspondance. July 1995.

Quentmeyer, Richard J. "Rocket Combustion Chamber Life-Enhancing Design Concepts," AIAA 90-2116, AIAA/SAE/ASME/ASEE 26th Joint Propulsion Conference, Orlando FL, 16-18 July 1990.

Rousar, Donald C. Engineer, Aerojet Corporation, Sacramento CA. Personal Correspondence. June 1995.

Schneider, P. J. Conduction Heat Transfer. Cambridge: Addison-Wesley Publishing Company Inc., 1955.

Sucec, James. Heat Transfer. Dubuque: Wm. C. Brown, Publishers, 1985.

Whitaker, Stephen. "Forced Convection Heat Transfer Correlations for Flow in Pipes, Past Flat Plates, Single Cylinders, Single Spheres, and for Flow in Packed Beds and Tube Bundles," AIChE Journal, Vol 18, pp 361-371, March 1972.

Vita

Jay A. Landis [redacted]. He graduated from the United States Air Force Academy in May 1989. He entered Euro-NATO Joint Jet Pilot Training at Sheppard AFB, Texas in September 1989 and graduated in October 1990. After medical reassignment, he was assigned to Falcon AFB, Colorado Springs, Colorado in April 1991. There he was the Lead Engineer Evaluator for the 4th Space Operations Squadron until his assignment to the Air Force Institute of Technology (AFIT). He began his Master's of Science program at the AFIT School of Engineering in May 1994.

[redacted]

REPORT DOCUMENTATION PAGE

Form Approved
OMB No. 0704-0188

1. AGENCY USE ONLY *(Leave blank)*	2. REPORT DATE	3. REPORT TYPE AND DATES COVERED
	December 1995	Master's Thesis

4. TITLE AND SUBTITLE

NUMERICAL STUDY OF A TRANSPIRATION COOLED ROCKET NOZZLE

5. FUNDING NUMBERS

6. AUTHOR(S)

Jay A. Landis, Captain, USAF

7. PERFORMING ORGANIZATION NAME(S) AND ADDRESS(ES)

Air Force Institute of Technology
2750 P Street
WPAFB, OH 45433-7126

8. PERFORMING ORGANIZATION REPORT NUMBER

AFIT/GA/ENY/95D-01

9. SPONSORING/MONITORING AGENCY NAME(S) AND ADDRESS(ES)

OLAC PL/RKCA
Terence Galati
4 Draco Drive
Edwards AFB, CA 93524-7160

10. SPONSORING/MONITORING AGENCY REPORT NUMBER

11. SUPPLEMENTARY NOTES

12a. DISTRIBUTION/AVAILABILITY STATEMENT

Approved for public release; distribution unlimited

12b. DISTRIBUTION CODE

13. ABSTRACT *(Maximum 200 words)*

This study proved that transpiration cooling provides a better cooling scheme than regenerative cooling for long operating duration, liquid-fueled rocket engine nozzles. This proof was made on the basis of maximum wall temperature. This study compared transpiration cooling to regenerative cooling in the throat region of the Space Shuttle Main Engine Main Combustion Chamber. The study also analyzed the effects of porosity, solid thermal conductivity, and porous sphere size on a porous wall made of packed spheres. The transpiration cooled nozzle operated 35% cooler than a regeneratively cooled nozzle, but the temperature gradient at the hot gas surface was 72 times greater than the regeneratively cooled nozzle.

14. SUBJECT TERMS

Sweat Cooling, Rocket Nozzles, Space Shuttle, Porous Metals, Nozzle Throats

15. NUMBER OF PAGES

92

16. PRICE CODE

17. SECURITY CLASSIFICATION OF REPORT	18. SECURITY CLASSIFICATION OF THIS PAGE	19. SECURITY CLASSIFICATION OF ABSTRACT	20. LIMITATION OF ABSTRACT
Unclassified	Unclassified	Unclassified	UL